

# **Study of residual stress distribution in relation to microstructure during deep cold rolling of Al6061**

*A dissertation submitted*  
in partial fulfilment of the requirements  
for the degree of

**Master of Engineering**  
in  
**Production Engineering**

by

**Rakesh Kumar**  
**Roll No: 801585021**

Under the Supervision of

**Dr. Gulshan Kumar**  
Assistant Professor



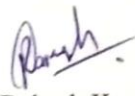
**MECHANICAL ENGINEERING DEPARTMENT**  
**THAPAR UNIVERSITY, PATIALA**

**July, 2017**

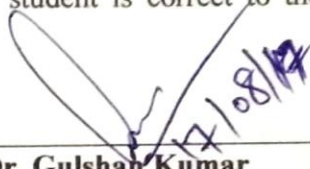
# Certificate

I hereby declare that the thesis entitled “**Study of residual stress distribution in relation to microstructure during deep cold rolling of Al6061**”, is an authentic record of my work carried out as per requirements for the award of the degree of **Master of Engineering in Production Engineering** under the supervision of **Dr. Gulshan Kumar** Assistant Professor, Mechanical Engineering Department, Thapar University, Patiala during July 2016 to July 2017. No part of the matter embodied in this report has been submitted to any other university or institute for the award of any degree.

Date: 17/08/2017

  
Rakesh Kumar

It is certified that the above statement made by the student is correct to the best of our knowledge and belief.

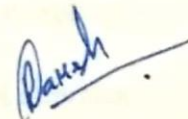
  
\_\_\_\_\_  
**Dr. Gulshan Kumar**  
Assistant Professor  
Mechanical Engineering Department  
Thapar University, Patiala - 147004

# Acknowledgement

I would like to express my deep sense of gratitude and a very sincere thanks to my supervisor **Dr. Gulshan Kumar**, Assistant Professor, at Mechanical Engineering Department, Thapar University, Patiala for his sincere and invaluable guidance which helped me in the accomplishment of this report in the present form. Their dynamic and diligent enthusiasm has been highly instrumental in keeping my spirits high. Their flawless and forthright suggestions blended with an innate intelligent application have crowned my task with success.

I am also thankful to **Prof. Indradev Samajdar**, Department of Metallurgical Engineering and Materials Science, IIT Bombay for allowing me to carried out my measurements at OIM & Texture lab. I also thank **Mr. Khushal Thool**, Research Scholar at IIT Bombay for his help in the measurement of residual stress and microstructure for carrying out my thesis work.

I would like to thank my friends especially my classmates ME (production), Thapar University, Patiala for their immense support during my thesis work.



Rakesh Kumar

Roll No.: 801585021

# List of Figures

---

Figure 1.1	Compressive and Tensile Residual Stresses behavior.	1
Figure 1.2	Two phases ‘composite’ material system describing the formation of residual stresses.	2
Figure 1.3	Multiple origin of residual stress.	2
Figure 1.4	a) Macroscopic b) Microscopic.	3
Figure 1.5	Atomistic origin of residual stress.	3
Figure 1.6	Micro-stress and Macro-stress (the average of local or micro-stresses).	4
Figure 1.7	Deep Cold Rolling Process.	5
Figure 2.1	Effect of (a) depth and (b) roughness as comparison to another surface treatment.	10
Figure 2.2	Conical Rounded Tool.	11
Figure 2.3	(a) Laser cladding technique, (b) Deep surface rolling technique.	12
Figure 2.4	Optical picture of (a) Low force, (b) High force deep rolling surface and (c) Shot peened surface.	13
Figure 2.5	Simulation Modal of Shot Peening and Deep Rolling.	14
Figure 2.6	Microhardness and Residual Stress Depth profile.	14
Figure 2.7	Deep rolling with a) overlapping b) Coefficient of friction c) varying rolling force d) Vibration on Workpiece.	15
Figure 2.8	Influence of material strength on the bending fatigue strength of unrolled deep rolled of 37CrS4.	16
Figure 2.9	Residual stresses in longitudinal (ax) and circumferential direction of the rods (tan) of the samples 1 to 6 after deep rolling with the parameters given in table. 3 and plotted as function of the distance from the surface.	17
Figure 2.10	Effect of temperature on deep rolled material residual stress and hardness.	18
Figure 2.11	X-ray diffraction concept.	19
Figure 2.12	Longitudinal stress distribution before and after cold rolling.	20
Figure 3.1	Deep rolled aluminium (Al 6061) plate.	22
Figure 3.2	Diamond cutter and Cut sample of Al6061.	23
Figure 3.3	Deep rolling setup.	24
Figure 3.4	Tensile Testing.	24
Figure 3.5	Sample set-up and GIXRD Panalytical™ setup.	25
Figure 3.6	Abrasive papers and setup of (polishing).	25
Figure 3.7	Electro-polishing.	26
Figure 3.8	Wire EDM.	26
Figure 3.9	EBSD setup.	27
Figure 3.10	Surface Roughness Testing Machine.	28

Figure 4.1	A three dimensional, Elasto-plastic finite element model for 0.5 mm, 1 mm, 1.5 mm and 2 mm deep rolled.	30
Figure 4.2	Meshing of sheet.	31
Figure 4.3	Mesh sensitivity analysis.	32
Figure 5.1	EBSD results.	34
Figure 5.2	EBSD data for different deep rolled depth 0, 0.5, 1, 1.5, 2 mm (a) Grain size and (b) kernel average misorientation (KAM).	35
Figure 5.3	Residual stress signatures as a function of thickness: (a) $\sigma_{11}$ and (b) $\tau_{12}$ .	36
Figure 5.4	Residual stress gradient in longitudinal direction (LD).	37
Figure 5.5	Residual stress gradient in transverse direction (TD).	38
Figure 5.6	Shear stress gradient.	39
Figure 5.7	Relationship of reaction force with time.	39
Figure 5.8	Average surface roughness.	40

# List of Tables

---

Table 1.1	Applications of residual stress.	5
Table 1.2	Aluminium Alloys.	7
Table 2.1	Effect of parameters on deep rolled condition.	17
Table 3.1	Chemical composition of Aluminium alloy (Al6061).	21
Table 4.1	Plastic flow stress.	31

# Symbols

---

$\sigma$  = stress in general

$\mu$  = coefficient of friction

$E$  = modulus of elasticity, N/mm<sup>2</sup>

$s_f$  = the stress in the direction of x-ray beam tilt angle

$D_d/d_o$  = the atomic spacing divided by the unstressed atomic spacing i.e., strain

$y$  = the relative x-ray beam tilt angle

# Acronyms

EBSD = electron backscattered diffraction

FE = finite element analysis

LD = longitudinal direction

TD = transverse direction

COF = coefficient of friction

GIXRD = grazing incidence x-ray diffraction

# Abstract

---

The main objective of the present dissertation was to observe the residual stress distribution on the surface of the material during deep cold rolling. Deep cold rolling (DCR) is surface treatment technique and it is used to modify surface properties. During DCR, deformation takes place at the surface and sub surface of specimen which leads to surface finishing and increase its fatigue strength. The observed residual stresses were correlated with the microstructural features. The residual stress and microstructure characteristics were examined using X-ray diffraction and EBSD technique respectively. It was found that deep cold rolling leads to microstructure refinement and lowering of residual stress. The compressive residual stresses were higher on the sub-surface compared to top surface of the material. These stresses reduced with penetration depth at a particular deep rolled state. To confine such stress gradients, a 3-dimensional, elastic-plastic FE (finite element) model was developed. An agreement has been observed between the experimental and the simulated residual stress distributions.

Keywords: Al 6061, Deep Cold Rolling (DCR), Grazing Incidence X-Ray Diffraction (GIXRD), Electron Back Scatter Diffraction (EBSD), Finite Element Modelling (FEM) Method.

# Table of Contents

	<b>Page No.</b>
<i>Certificate</i> .....	<i>i</i>
<i>Acknowledgement</i> .....	<i>ii</i>
<i>List of Figures</i> .....	<i>iii</i>
<i>List of Tables</i> .....	<i>v</i>
<i>Symbols and Acronyms</i> .....	<i>vi</i>
<i>Abstract</i> .....	<i>vii</i>

## **Chapter 1**

<b>INTRODUCTION</b> .....	<b>1-9</b>
1.1 Introduction .....	1
1.2 Residual Stress .....	1
1.2.1 Origin of Residual Stress .....	2
1.2.2 Classification of Residual Stress .....	4
1.2.3 Application of Residual Stress .....	4
1.3 Deep Cold Rolling .....	5
1.3.1 Application of Deep Cold Rolling .....	6
1.4 Aluminium .....	6
1.4.1 Applications of Aluminium Alloys .....	7
1.5 Motivation .....	8
1.6 Summary .....	8
1.7 Organization of Report .....	9

## **Chapter 2**

<b>LITERATURE REVIEW</b> .....	<b>10-20</b>
2.1 Introduction .....	9
2.2 Literature Review .....	9
2.3 Summary of Literature Review .....	20
2.4 Gaps in the Existing Literature .....	20

## **Chapter 3**

<b>DESIGN OF STUDY</b> .....	<b>21-28</b>
3.1 Introduction .....	21
3.2 Starting material .....	21
3.3 Methodology .....	22
3.4 Machines and Equipment .....	22
3.4.1 Diamond Cutter .....	22
3.4.2 Deep Cold Rolling Setup .....	23
3.4.3 Tensile Testing Machine .....	23
3.4.4 GIXRD- Grazing Incidence X-Ray diffraction .....	24

3.4.5 Polishing .....	25
3.4.6 Electro-polishing .....	25
3.4.7 Wire EDM Set-up .....	26
3.4.8 Electron Back Scatter Diffraction (EBSD) .....	26
3.4.9 Surface Roughness Testing .....	27
3.5 Summary of this chapter .....	28

## **Chapter 4**

### **FINITE ELEMENT MODELLING .....29-32**

4.1 Physical Description of FE Model .....	29
4.2 Numerical Formulation .....	30
4.3 Material Model .....	31
4.4 Boundary and Contact Conditions .....	31
4.5 Mesh Sensitivity .....	32

## **Chapter 5**

### **RESULTS AND DISCUSSION .....33-40**

5.1 Introduction .....	33
5.2 Surface Microstructural Development .....	33
5.2.1 Gradients in grain structure .....	33
5.2.2 Gradients in residual stress .....	35
5.3 Process Characterization via Finite Element Simulations .....	37
5.3.1 Evolution of surface residual stresses .....	37
5.4 Surface Roughness .....	40

## **Chapter 6**

### **CONCLUSIONS AND SCOPE OF FUTURE WORK .....41**

6.1 Conclusions.....	41
6.2 Scope of Future Work.....	41

### **References .....42**

# Chapter 1

## Introduction

---

### 1.1 Introduction

The present chapter provides a brief introduction about the deep cold rolling process, the origin of residual stress, their importance and finally the usage and the application of the aluminium alloys, the material chosen for the present work.

### 1.2 Residual Stress

The stresses remained in a body in the absence of any external agency are to be considered as residual stresses. In other words, the stress exists in a structural material or component without the application of any external load are called as residual stress [1]. These can be beneficial or detrimental. For example, shot peening imparts compressive residual stresses on the surface of the component, improves the fatigue strength of the material [2]. Undesirable residual stresses are tensile residual stress can lead to increase crack propagation, distortion, premature failures in components [3]. These stresses are usually harmful because its make the surface of the body brittle and decrease the mechanical strength [4].

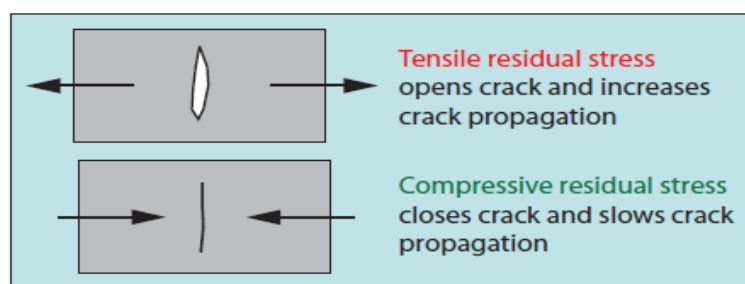


**Figure 1.1:** Compressive and Tensile Residual Stresses behaviour [5].

The schematic representing the creation of residual stress in a two-phase composite material system is shown in figure 1.2 [6]. The phase 'a' subjected to elastic deformation, however, the phase 'b' experienced an elastic-plastic deformation (figure 1.2a). After removal of the load, phase 'a' regain its original position and phase 'b' strained by  $d\varepsilon_p$  as shown in figure 1.2(b). On the other hand, figure 1.2(c) shows the real situation of unloading the two-phase

material system when both are joined together. The phase 'a' is extended by 'b', which in turn phase 'b' is compressed by 'a' [6].

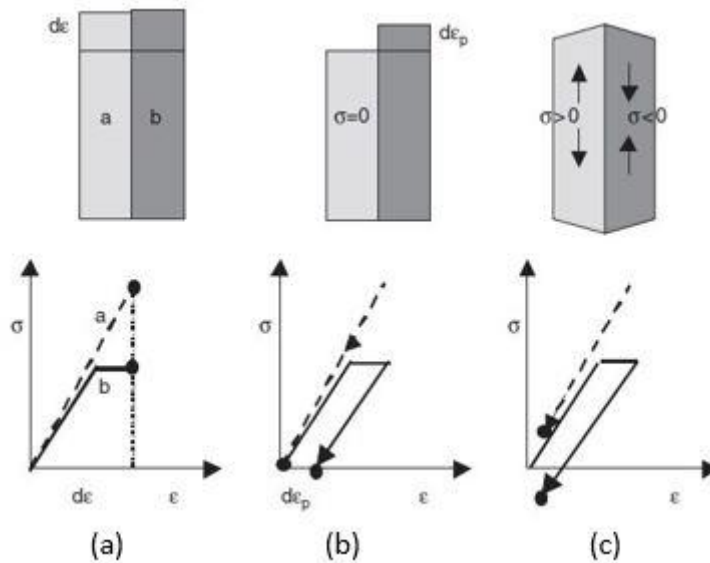


**Figure 1.2:** Two phase 'composite' material system describing the formation of residual stresses [6].

### 1.2.1 Origin of Residual Stress

The residual stresses can originate from defects (vacancies, dislocation, voids, cracks etc.), phase transformation and thermal origin as shown in figure 1.3 [7].

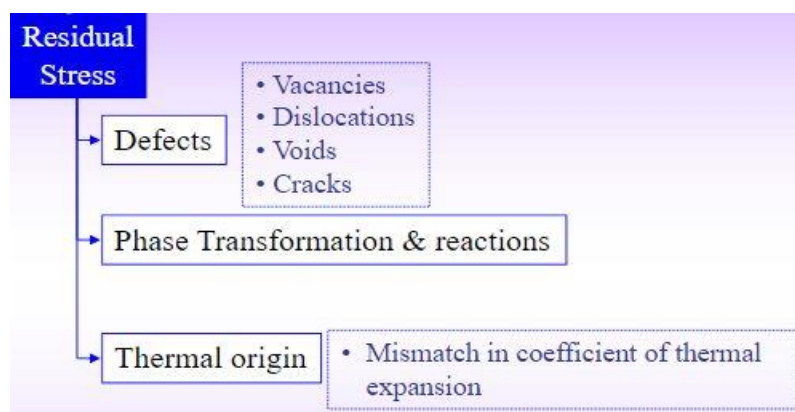


**Figure 1.3:** Multiple origin of residual stress [7].

The mismatch due to interplanar spacing and the constraints to retain that mismatch is the origin of any kind of stresses [6]. These can be of macroscopic or microscopic levels. For instance, riveting of two plates, bending of a bar and shot peening as shown in figure 1.4a

considered as macroscopic stresses [6]. On the other hand, the stresses induced in phase transformation of iron-based alloys are considered as microscopic (figure 1.4b) [6].

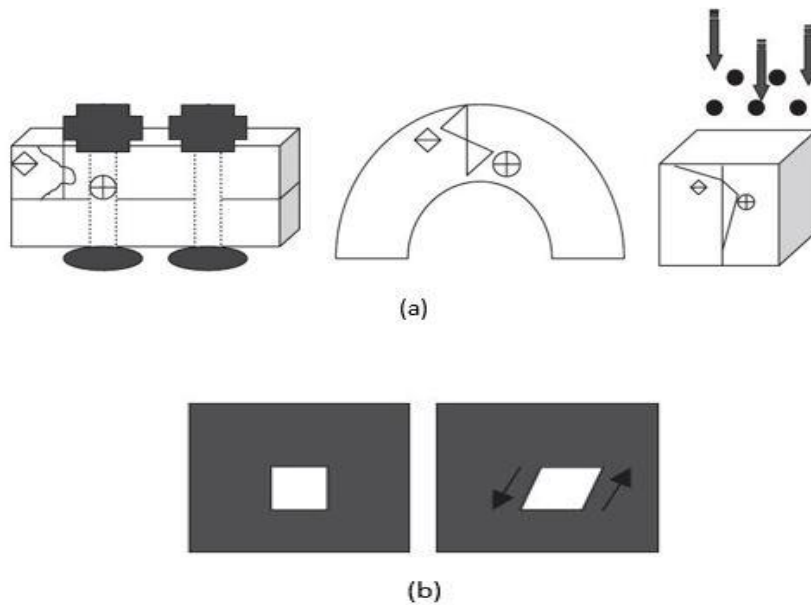


**Figure 1.4:** a) Macroscopic b) Microscopic [6].

The creation of residual stresses can be through a schematic of the deformation of an unreformed lattice structure (figure 1.5). The deformation lead to change in interplanar spacing or may induce the defects in the lattice. The former may remain in the body due to neighbouring constraints after the removal of external load. This is called as residual stress. For example, the interplanar spacing changes from  $d_0$  to  $d_1$  (figure 1.5) with the application of force. However, it remained in the body as lattice defects (dislocations) after the removal of imposed forces [6].

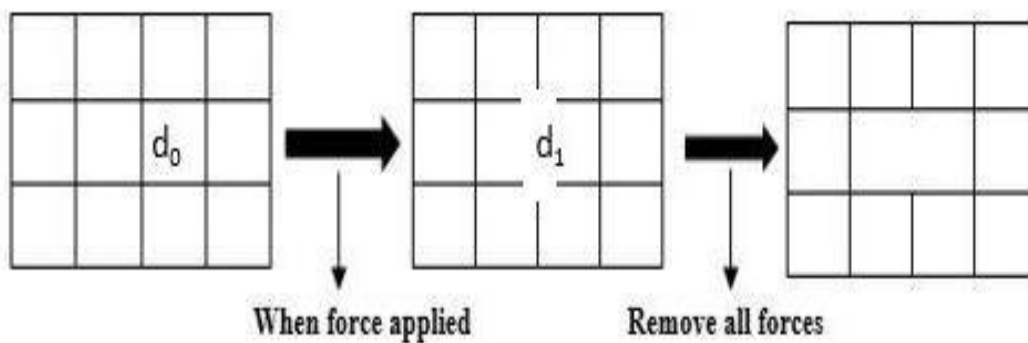


**Figure 1.5:** Atomistic origin of residual stress [6].

## 1.2.2 Classification of Residual Stress

Residual Stress mainly categorized as shown in figure 1.6 [8]:

- 1) Micro-stresses
  - 2) Macro-stress
- 1) Micro-stress: The stresses differ in grains due to existence of inclusion, dislocation, faults are micro stresses. This stress can also differ between the grains because each grain direction contains definite properties of elasticity and plasticity [8].
  - 2) Macro-stress: Macro stress is the average of stress generated in each grain [8].

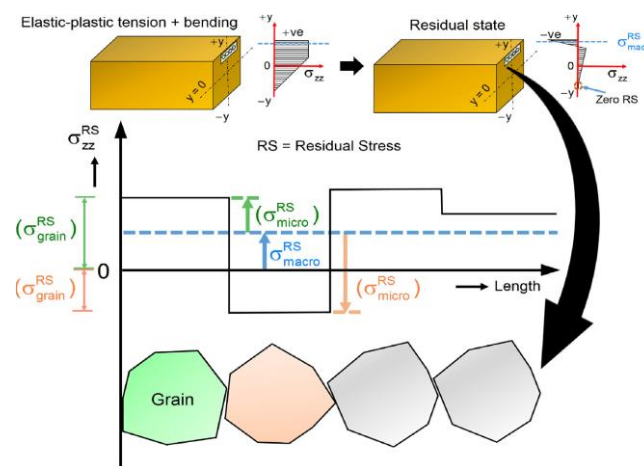


**Figure 1.6:** Micro-stress and Macro-stress (the average of local or micro-stresses) [8].

## 1.2.3 Applications of Residual Stress

Residual stress is very important for material to increase surface strength, fatigue strength, surface finish etc. The compressive residual stress progressively used in automobile (wheel flange) [15], propeller blade [9], turbine blade [2] (it increases the blade surface fatigue strength to resist hitted high air and water pressure) etc.

The various applications of residual stresses are shown in Table 1.1.

**Table 1.1:** Applications of residual stress.

S.No.	Application	Type of Residual Stress	Author
1.	Crank Shafts or Shaft Fillets	Compressive	J. Liou [10]
2.	Turbine Blades	Compressive	G.H. Majzoobi [2],
3.	Propeller Blades	Compressive	T.Yentzer [9]
4.	Wheel Flange	Compressive	I. Altenberge [17]

### 1.3 Deep Cold Rolling

Deep Cold Rolling (DCR) is a surface treatment technique to improve the fatigue strength of materials by inducing a compressive residual stress on the surface of the component. This is performed using a roller or ball type instrument as shown in figure 1.6. As a result of the contact of a roller or a ball with the surface of a component, a longitudinal groove is created which is accompanied by a plastic region followed by an elastic zone. Upon the separation of the roller, the recovery of elastic zone creates a large compressive residual stress on the surface. A number of parameters such as rolling pressure, coefficient of friction, roller velocity can severely influence the deep rolling process, and consequently the surface residual stress provided by rolling force is the important one [11].

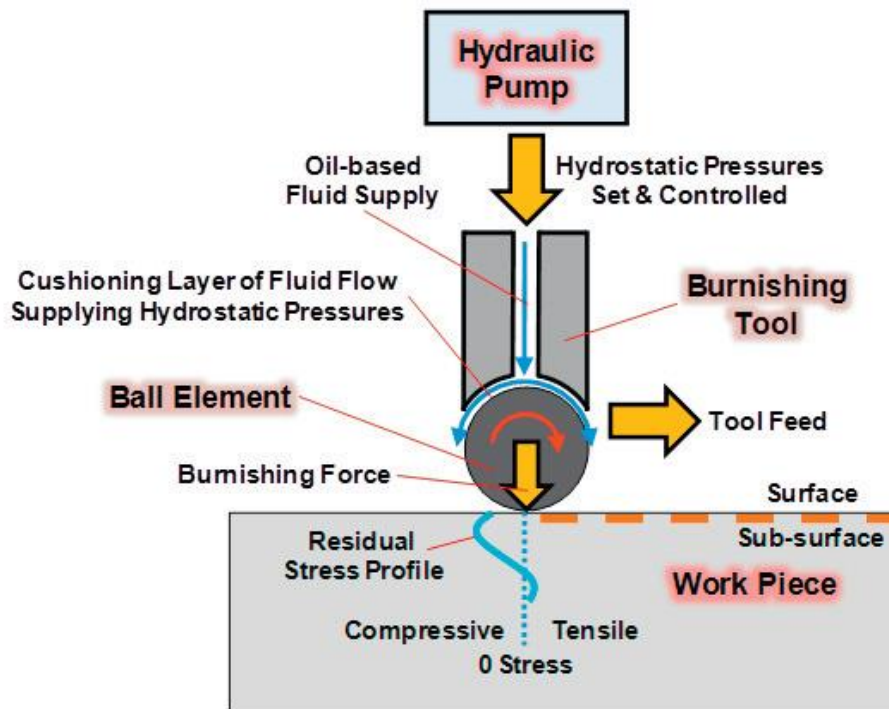


**Figure 1.7:** Deep Cold Rolling Process [11].

### 1.3.1 Application of Deep Cold Rolling

The Deep Cold Rolling technique is widely used in the automobile industry (in particular crankshafts and shaft fillets [10], turbine blades [2], wheel flange, turbine disk, compressor fan blade [17], in aero-space industry, railway axles etc. The process is commonly adopted to improve the resistance to wear, decrease stress corrosion cracking etc. Mostly, it is used to improve the fatigue strength, decrease crack propagation, surface finish of highly stress metallic component in an aero-space engine [17].

## 1.4 Aluminium

The first solidified aluminium was discovered in 1845 by a German Chemist, Hans Christian Oersted [12]. Aluminium is a chemical element with symbol 'Al' and atomic number 13 [13]. It is light in weight, non-magnetic in nature, ductile and less expensive compared to other materials such as titanium, chromium etc. The density of aluminium is very low (30%-35%) than iron and copper. It also gives high specific strength and stiffness. Aluminium alloys are basically used for their corrosion resistance because it develops a natural passivating oxide layer, approximately 2 nm thick, which acts as a buffer between the material and the environment [14].

The following properties of aluminium alloys make them suitable for the commercial purposes:

1. Aluminium is a good thermal and electrical conductor [14].
2. Many industry preferred aluminium due to its low density and less price, for example, aircraft industry uses aluminium for manufacturing the aircraft body [14].
3. Al has an FCC structure with 12 {111} [110] slip system. The high no. of the slip system allows for the material to be ductile [14].
4. Aluminium alloy can be divided into many categories as shown in table 1.2 [15].
  - a) Alloys which attain the strength by work hardening are the 1xxx, 3xxx, 4xxx and 5xxx series [14].
  - b) Alloy which attain the strength by heat treatment are the 2xxx, 6xxx, 7xxx and 8xxx series [14].

**Table 1.2:** Aluminium Alloys [15]

Al Alloys	Workability	Weldability	Machining	Corrosion Resistance	Heat Treating	Strength	Application
Al 1100	Excellent	Excellent	Good	Excellent	No	Low	Metal Spinning
Al 2011	Good	Poor	Excellent	Poor	Yes	High	General Machining
Al 2024	Good	Poor	Fair	Poor	Yes	High	Aerospace Application
Al 3003	Excellent	Excellent	Good	Good	No	Medium	Chemical Equipment
Al 5052	Good	Good	Fair	Excellent	No	Medium	Marine Application
Al 6061	Good	Good	Good	Excellent	Yes	Medium	Structural Application
Al 6063	Good	Good	Fair	Good	Yes	Medium	Architectural Application
Al 7075	Poor	Poor	Fair	Average	Yes	High	Aerospace Application

### 1.4.1 Application of Aluminium Alloys

Aluminium alloys used in various industrial application on the basis of its light weight, resistance to corrosion, better ductility etc. [16].

- a) **Aerospace:** Aerospace industry required a stronger, light weight structure material. Because of these two-leading property aluminium alloys are number one material in the sky as comparison to other materials.
- b) **Automotive:** In automotive industry, the various parts such as chassis, bodies, castings for engine, transmission, wheel applications, heat exchangers and radiators et., are made by aluminium alloys due to their high strength, light weight, low cost and resist to corrosion etc.
- c) **Marine:** The popularity of aluminium increasing in fabricating marine due to light weight and corrosion resistance in water. It is also used in superstructures like pleasure boats, bridges, passenger ships and merchant ships.

- d) **Rail:** Due to their light weight, higher corrosion resistance and durability, the demand of aluminium alloys is increasing in rail transport applications.
- e) Aluminium is mostly used in modern structural application like for window frames, glass supports, partitions and decorations etc. because of its low maintenance, cost is low and stand up in weather (not rusty) etc. These all features attract architects and builders use aluminium in hospitals, universities, office buildings, industrial buildings and private houses etc.

## 1.5 Motivation

One of the main challenges for aircraft, automobile industry, structure application is to reduce the impact of high pressure air, water, oil. A lot of research has been done on minimizing the high air, water pressure and other environmental effect on the surface of specimen, which can be achieve by surface treatment technique like shot peening, laser shot peening, laser hardening etc. Due to this, materials with higher surface fatigue strength are preferred. Aluminium has maximum strength, light weight and low cost, high corrosion resistance, and the ability to stand for long time in environment. It is used in the engine applications such as turbine blades, propeller blades, wheel flange, connecting rod etc. The residual stresses are induced on the surface of turbine blades, propeller blades, wheel flange, connecting rod

The various mechanical and thermal processes, such as shot peening, laser shot peening, laser hardening etc., results into the creation of minimum residual stresses and higher surface roughness, minimum fatigue life. To give a useful fatigue life and high surface finishing, the critical blades can be deep cold rolled to bring the compressive residual stresses up to a reasonable depth [2]. The residual stress has been calculated over the surface till now, but it has not been correlated with microstructural features in the past. This gives me the motivation to plan for the proposed research work “Study of residual stress distribution in relation to microstructure during deep cold rolling of Al6061”.

## 1.6 Summary

This chapter started with a brief introduction of residual stress. Further, different types of stresses, its origin and commercial applications have been explained. An emphasize on aluminium and its alloys have been given being the material used for the present research work. The deep cold rolling process used to deform the surface of aluminium alloy (Al6061)

alloy in the present work has been also introduced briefly in this chapter. In the last section motivation has been briefly introduced.

## **1.7 Organization of report**

This report is divided into six main chapters. In Chapter 1, general introduction of the work is explained briefly. Chapter 2 contains the comprehensive literature review related to the problem along with general theory of mechanical properties of aluminium. Chapter 3 describes the characterization techniques used for carrying out the experimental work. Chapter 4 contains the details about the finite element modelling of the deep cold rolling. The chapter 5 includes the results and discussion of the residual stress gradient during deep cold rolling of aluminium alloy. The experimental results were further validated with the FE Simulated results. The chapter 6 summarized the present work and provided the future scope for further research.

# Chapter 2

## Literature Review

---

### 2.1 Introduction

In this chapter, the literature of different processes as per the applications has been discussed. Also, the experimentation done till now to obtain the effects of different parameters on residual stress, fatigue strength and surface roughness value have been reported.

### 2.2 Literature Review

**Altenberger [17]** worked on deep rolling surface treatment technique and shows the effect of deep rolling on residual stress and surface roughness at a material as comparison to other surface treatment technique as shown in figure 2.1. And benefits of deep rolling surface treatment technique is resist to corrosion, improve wear and superfinishing of surfaces at a specimen.

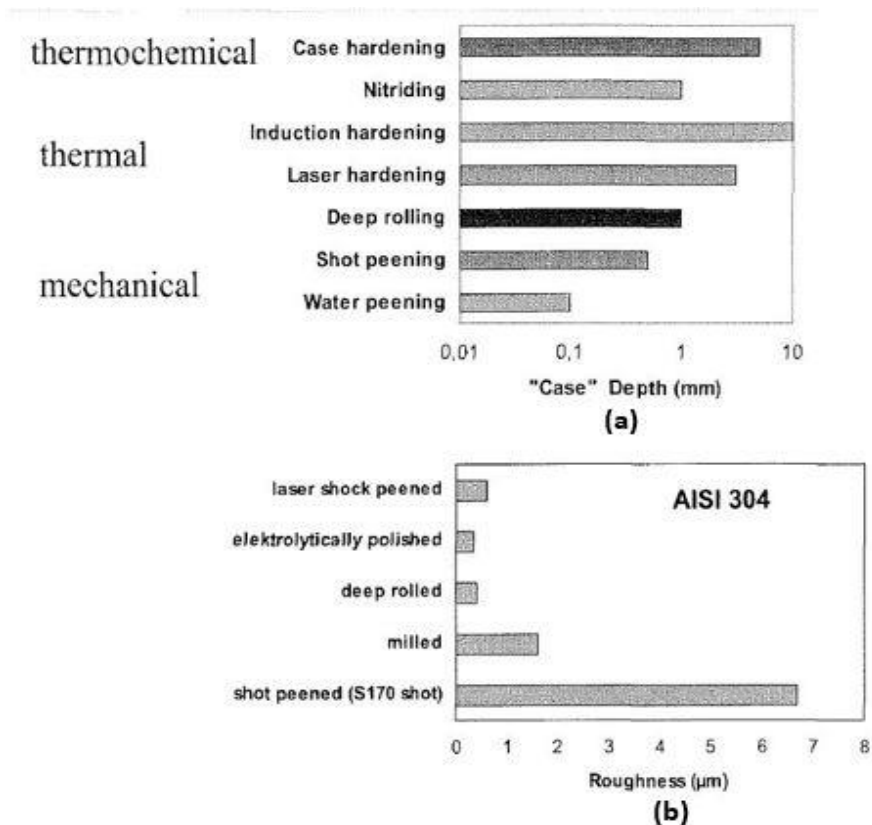


**Figure 2.1:** Effect of (a) depth and (b) roughness as comparison to another surface treatment [17].

**Beghinia et al. [18]** worked on residual stress induced in high strength aluminium alloy (Al 7075-T6) by deep cold rolling conical and rounded tool (fig. 2.2) and its depend on many factors like feed rate, roller speed, roller feed, roller shape, applying force by roller etc. Feed of roller affects the upper surface of the component, but does not affect the large depth or says subsurface. But combination of rolling force and rolling feed effect surface of the hardness, if rolling force is maximum and feed is minimum then surface hardness is maximum. The creation of deep compressive residual stress is influenced by the feed, if feed low maximum deep (up to 1mm) residual stress create. Deep cold rolling device can be easily used with common machine tool like milling and lathe machine. In this paper also discussed about a compressive residual stress is increase when force increase. Compressive nature of residual stress converts into tensile nature when going down depth up to 1mm measured.

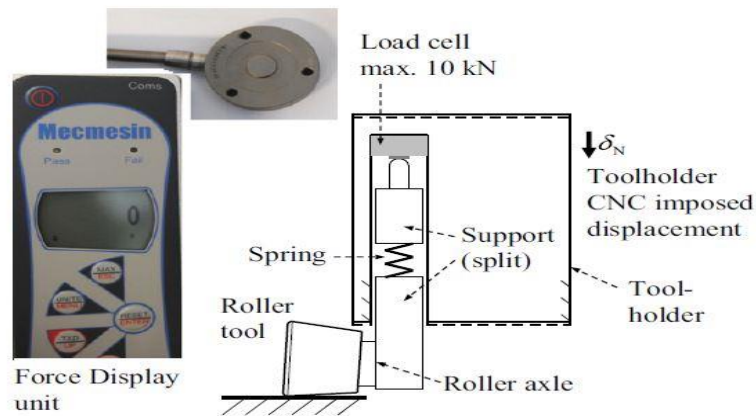
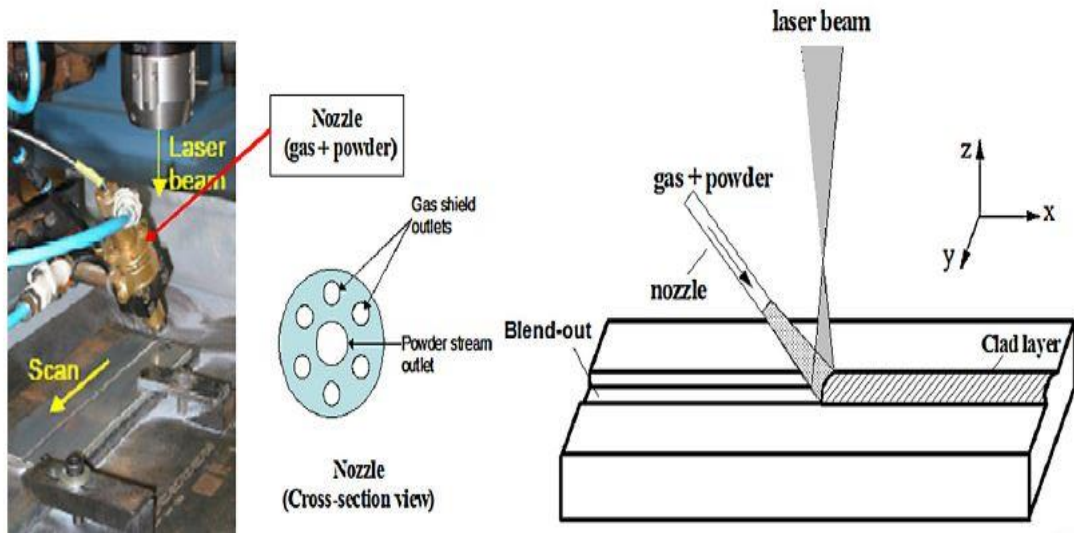


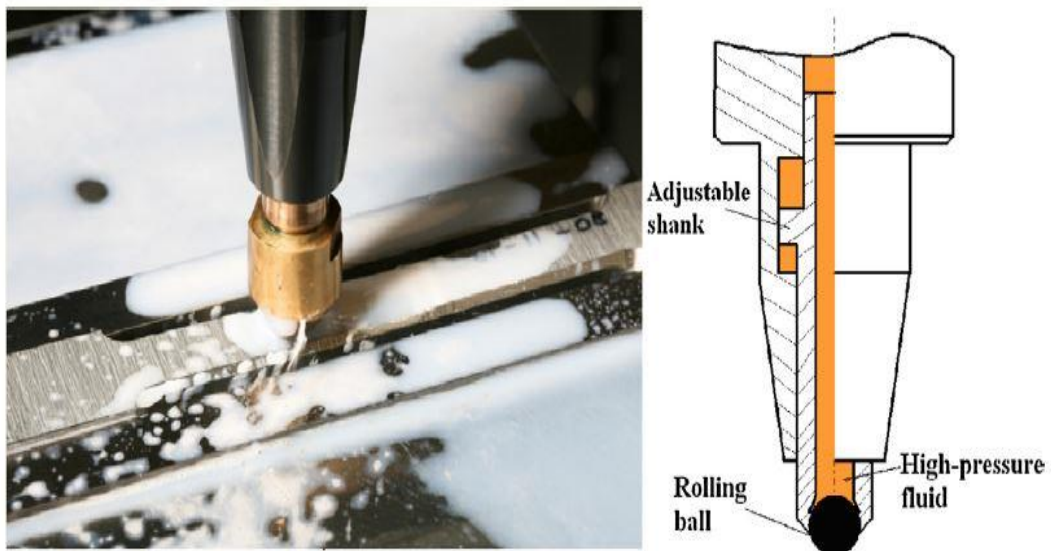
**Figure 2.2:** Conical Rounded Tool [18].

**Zhuanga et al. [19]** performed the experiment on deep surface rolling post-repair enhancement technology was applied on the laser cladding surface of high strength aluminium alloy (Al 7075-T651) material to increase fatigue life. Deep surface rolling creates deep compressive residual stress in the surface of aircraft metallic structure to increase its fatigue life. And aircraft structure repaired by the laser cladding technology is very costly, because of this reason deep surface rolling technique used as an advanced post-repair. The surface of the laser cladding region was treated by deep surface rolling technique for Fatigue testing and it was found that deep surface rolling technique increase fatigue life as comparison to laser cladding. And also, deep compressive residual stress (depths more than 1.0 mm below) create by deep surface rolling as comparison to laser clad surface. Firstly, the deep surface rolling process create deep and high magnitude compressive residual stresses as

compared to the laser cladded material, then increased roughness on specimen (Al 7075-T651) by the deep surface rolled is also contribute to improving fatigue performance. First, laser cladding technique (fig. 2.3a) then deep surface rolling technique (fig. 2.3b) at the same surface of aluminium alloy (Al 7075-T651) is shown in figure 2.3.



(a)



(b)

**Figure 2.3:** (a) Laser cladding technique, (b) Deep surface rolling technique [19].

**Majzooobia et al. [2]** worked on improve fatigue resistance, fatigue life of aluminium 7075-T6 material by using roller or ball type (deep cold rolling) surface treatment technique as

compare to the shot peening technique. Deep Rolling is widely used in automobile industry (in particular crankshaft), in aero industry to improve the fatigue resistance or fatigue life of propeller blades and turbine blades etc. The results show, for low deep rolling force shot peening is superior then deep rolling and increases fatigue life of material 300% by shot peening technique. And another side for high deep rolling force, deep rolling increase fatigue life (around 700%) is more than shot peening. Optical picture of the low forced deep rolled surface (fig. 2.4a), high force deep rolled surface (fig. 2.4b) and shot peened surface (fig. 2.4c) is shown in figure 2.4. In deep rolling process fatigue strength is depend on the roller radius, feed of roller, rolling Load, coefficient of friction and material strength etc.

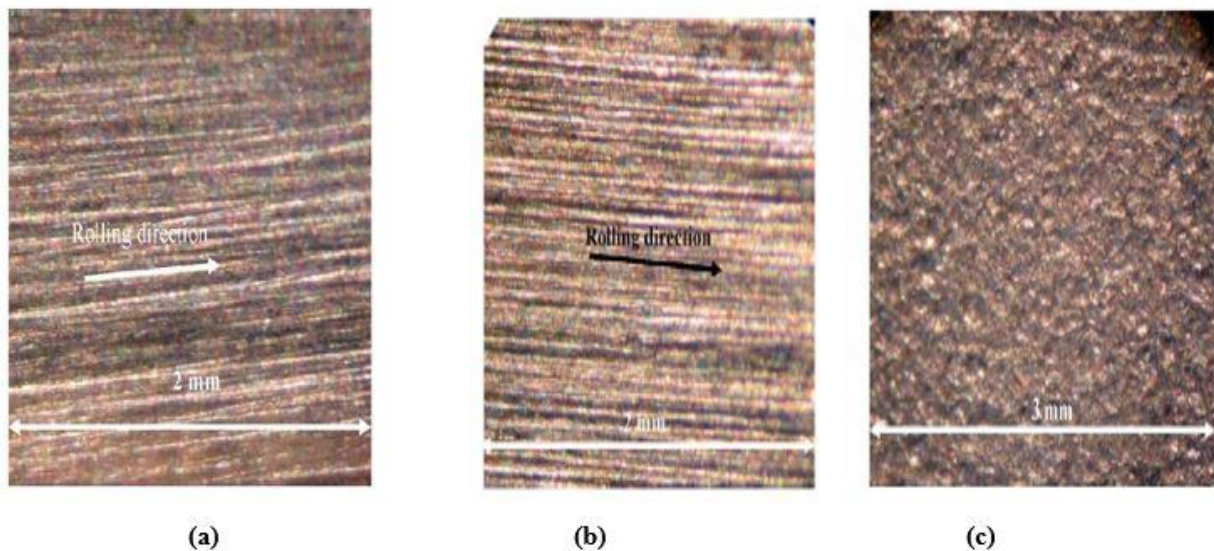


**Figure 2.4:** Optical picture of (a) Low force, (b) High force deep rolling surface and (c) Shot peened surface [2].

Numerical simulation of shot peening and deep rolling is also performed and simulated result compared with experimental work. The results indicate the deep cold rolling gives larger compressive residual stress than shot peened under the conditions considered in the simulations. A simulation modal of deep rolling and shot peening is shown in figure 2.5.

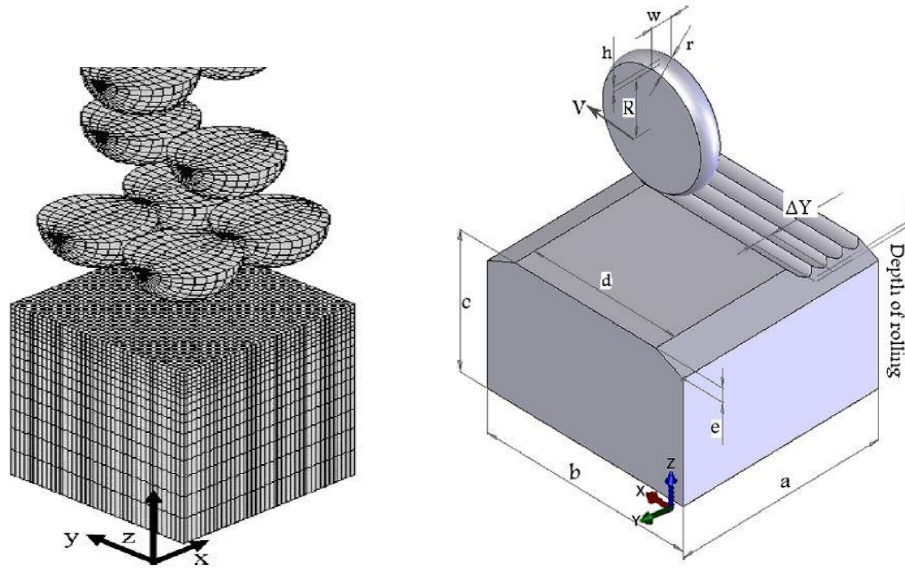


**Figure 2.5:** Simulation Modal of Shot Peening and Deep Rolling [2].

**Altenberger et al. [20]** worked on deep rolled aluminium alloy (Al 2024) at a different temperature (T4 and T6) and 100 bar rolling pressure. Deep rolling induced a depth profiles of microhardness, compressive residual stresses in aluminium alloy (Al 2024) and compare the results of T4 and T6 temperature as shown in figure 2.6.

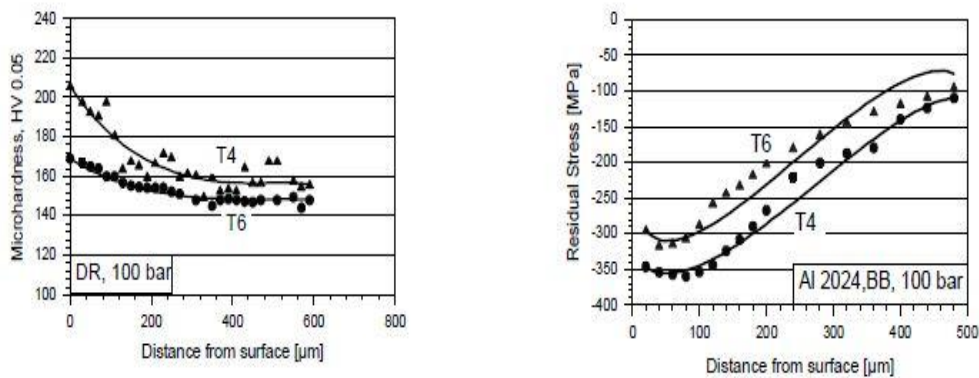


**Figure 2.6:** Microhardness and Residual Stress Depth profile [20].

**Manouchehrifar et al. [6]** worked on the simulation of deep rolling technique and show the effect of all parameters (overlapping of roller tracks on the surface, coefficient of friction in between roller and component, varying force and vibration of workpiece and tool) on

compressive residual stress (fig. 2.7) and improvement of the fatigue behavior of metallic components. Deep rolling is attractive technique because in this technique, it is possible to generate deep compressive residual stresses near surface. And another advantage of deep rolling is high strain hardening inside the surface layer of component.

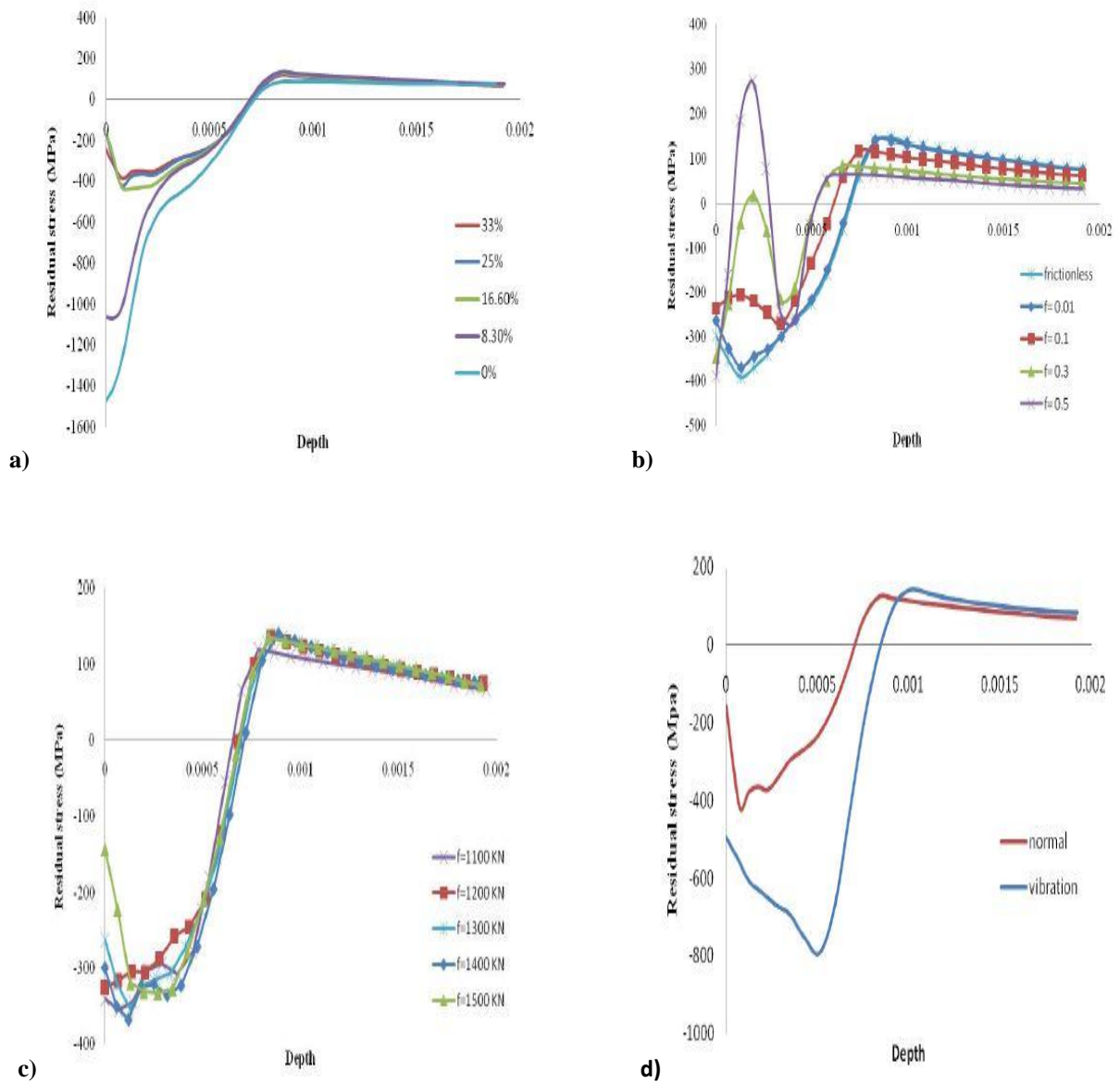


**Figure 2.7:** Deep rolling with a) overlapping b) Coefficient of friction c) varying rolling force d) Vibration on Workpiece [6].

**Kloos et al. [21]** discussed about a fatigue property of material is change by the influence of deep rolling condition deep rolling process fatigue strength is depend on the Roller Radius,

feed of roller, Rolling Load and material strength etc. In below figure 2.8 shows a size of roller or says different angle where roller give different type of result. And also in figure 2.8 shows a deep rolling increase rotating bending strength and tensile strength.

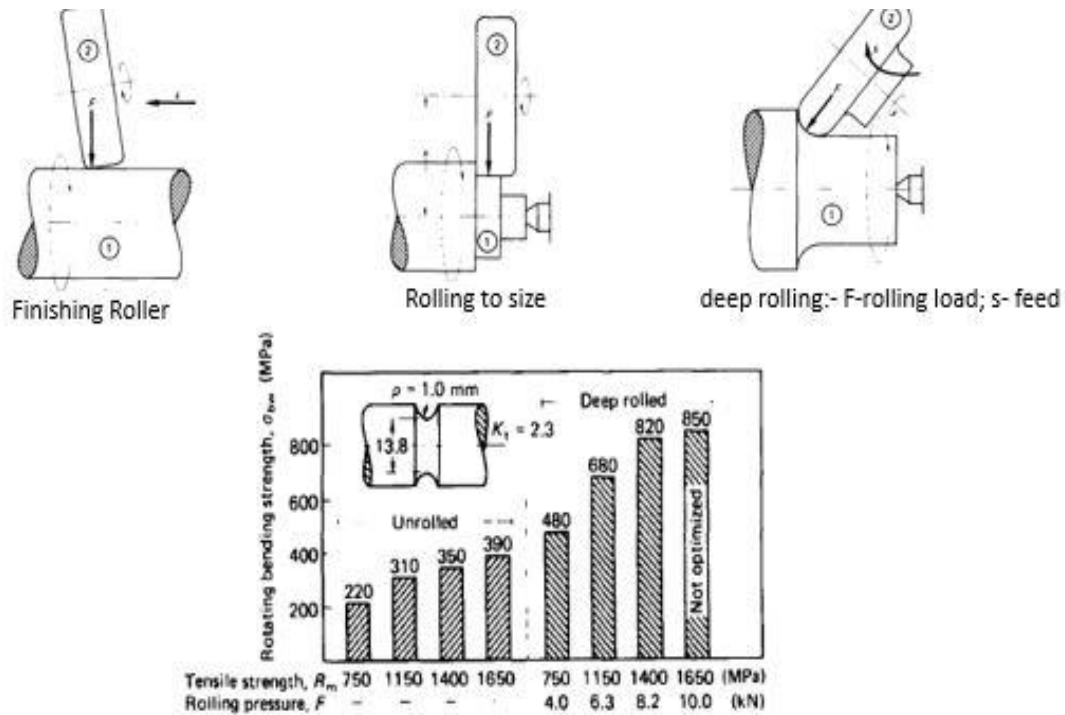


**Figure 2.8:** Influence of material strength on the bending fatigue strength of unrolled deep rolled of 37CrS4 [21].

**Eigenmann et al. [22]** It could be demonstrated that deep rolling allows to produce variations of depth distributions of residual stresses in a wide range by choosing the respective rolling parameters. In below figure 2.9 shows that a residual stress is at sample 6 with rolling pressure is 300bar with both longitudinal and circumferential direction. But in longitudinal direction compressive residual stress is two times more than circumferential direction. And in the Table 3 shows from sample 1 to 6 cross feed and deep rolling ball diameter is same but pressure is increase so residual stress also increases and surface roughness is decrease.

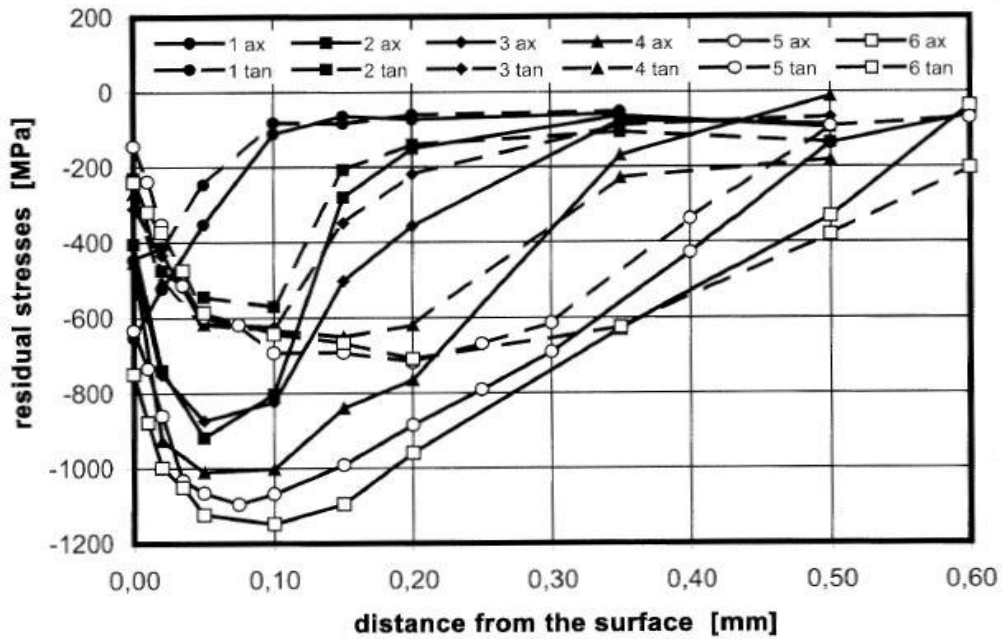


**Figure 2.9:** Residual stresses in longitudinal (ax) and circumferential direction of the rods (tan) of the samples 1 to 6 after deep rolling with the parameters given in table. 3 and plotted as function of the distance from the surface [22].

**Table 2.1:** Effect of parameters on deep rolled condition [22].

Sample No.	Cross feed (mm/rev.)	Deep Rolling ball diameter (mm)	Pressure (bar)	Average Surface Roughness $R_a$ ( $\mu\text{m}$ )
1	0.2	6	50	1.7
2	0.2	6	100	0.7
3	0.2	6	150	0.4
4	0.2	6	200	0.3
5	0.2	6	250	0.3
6	0.2	6	300	0.2

**Juijerm et al [23]** A effect of temperature on residual stress and surface hardness is shown in figure 2.10. At temperature 20°C compressive residual stress is maximum when temperature increase up to 250°C compressive residual stress minimum. So deep rolling is developed maximum compressive residual stress at cold process not heat treated. And hardness is change with temperature.

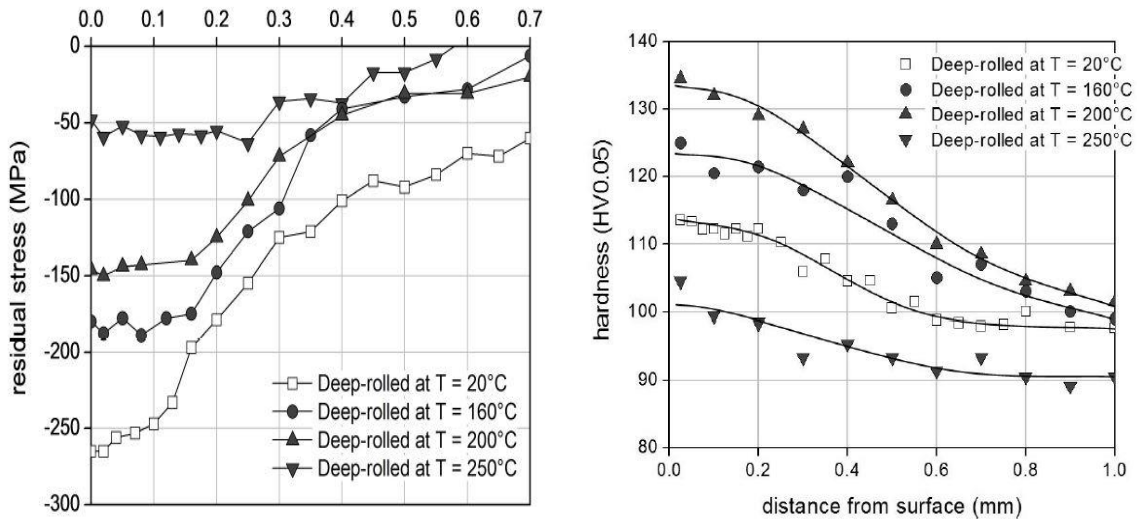
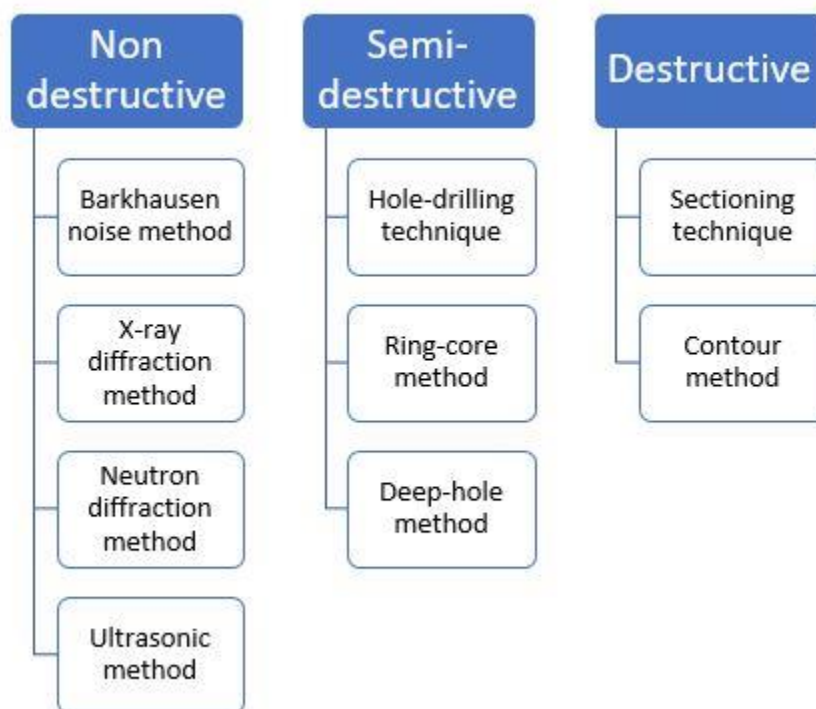


**Figure 2.10:** Effect of temperature on deep rolled material residual stress and hardness [23].

**Rosini et al. [24]** Residual stress measuring technique is Non-Destructive, Semi Destructive, Destructive. The destructive and semi destructive techniques, called also mechanical method such as Sectioning, contour, hole-drilling, ring-core and deep-hole are the principals destructive and semi destructive techniques used to measure residual stresses in structural members. Non-destructive methods include X-ray or neutron diffraction, ultrasonic methods and magnetic methods. These techniques usually measure some parameter that is related to the stress.



**Yentzer et al. [9]** The structural integrity of aluminium alloy propeller blades used on military and civil aircraft. Cold rolled introduce a compressive residual stress in surface of the appropriate magnitude and depth. The cold rolling process parameters were optimized (the resultant residual stress profile and the depth of the cold work-induced plasticity) by X-Ray Diffraction (XRD) residual stress measurement is shown in figure 2.11. Cold rolling process is a relationship between rotational speed and tool feed rates i.e., the load and residual stress linear up to the point that the surface is damaged by excessive force.

### X-Ray Diffraction(XRD) Technique

$$sf = Dd/d_0 / (\frac{1}{2} S_2 \sin 2y)$$

Where,  $sf$  = the stress in the direction of x-ray beam tilt angle,

$Dd/d_0$  = the atomic spacing divided by the unstressed atomic spacing i.e., strain,

$y$  = the relative x-ray beam tilt angle

$$\frac{1}{2} S_2 = (1 + n) / E \text{ (the x-ray elastic constant)}$$

X-ray diffraction concept.

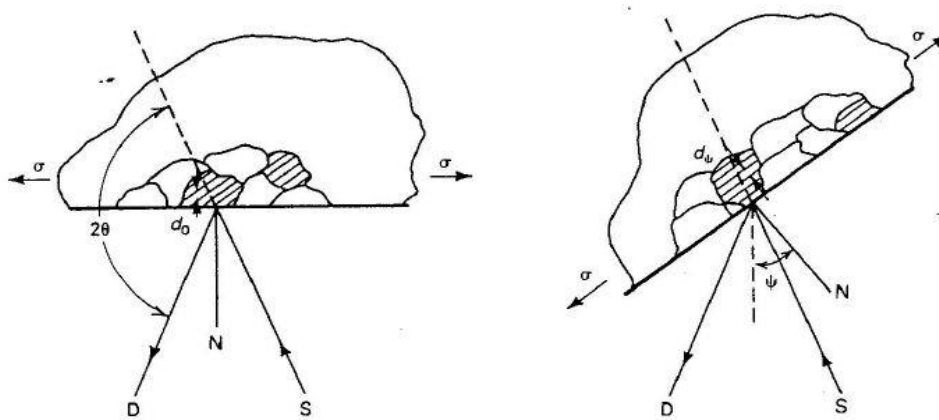


**Figure 2.11:** X-ray diffraction concept [9].

**Yong Ye et al. [25]** Residual stress are tensile on the surface of the aluminium alloy sheet and compressive inside when rolling reduction was small. Increase rolling reduction, the residual stress distributed more non-uniformly as shown in figure 2.12. Influence of rolling reduction, rolling velocity, friction coefficient and initial stress state on the residual stress value and distribution.

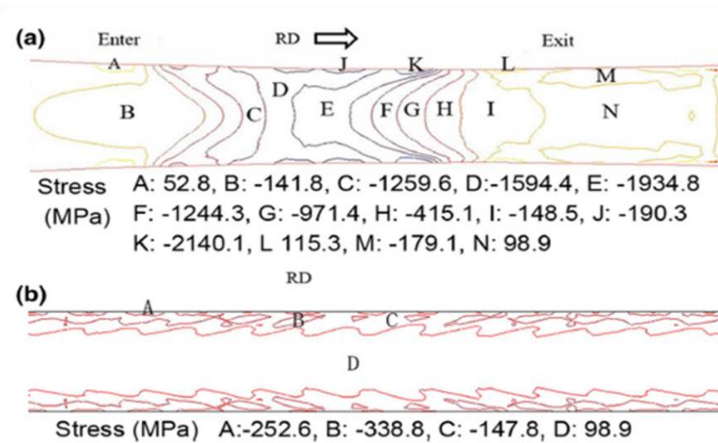


Figure 2.12: Longitudinal stress distribution before and after cold rolling [25].

## 2.3 Summary of the literature review

It was observed that deep cold rolling improved the surface fatigue strength, surface finishing and wear. It has been showed that high deep rolling pressure of cold working is improving fatigue life, surface finishing of the aluminum alloy. The strength effect by the different deep rolling parameters like COF, overlapping, varying pressure and load etc. Reason behind the deep cold rolling is increase surface compressive residual stress with high surface finishing.

## 2.4 Gaps in the existing literature

A past literature is available on the effect pressure, coefficient of friction, load of deep cold rolling on residual stress and surface roughness of aluminium. No work has been reported to study the correlation of residual stress and microstructure of aluminium alloy during deep cold rolling. The proposed research work is “*Study of residual stress distribution in relation to microstructure during deep cold rolling of Al606*”. However, the following limitations have been observed after a detailed literature review.

- Study of microstructures gradient during deep cold rolling in aluminum alloy has not been done yet.
- No work has been reported on experimentation of the effect of sensitive parameters (like overlapping of roller tracks on the surface, varying force and vibration of workpiece or tool) on compressive residual stress an aluminium alloys.
- Effect of compressive residual stress, surface roughness and surface hardness on corrosion rate during deep rolling of Al6061 has not been studied.

# Chapter 3

## Design of the Study

---

### 3.1 Introduction

This chapter discusses the overall design of the study which includes objective of the research work, the key issues, constituent materials of the alloy, and methodology. The chapter also covers the details of machines and equipment used for the experimental work.

### 3.2 Starting Material

For this experiment aluminium alloy is used (table 3.1), because it is very light material as compare to other like titanium, Ni, Fe etc. And it is used for structure application because its workability, weldability and machining is good, corrosion resistance is excellent and strength is medium as compare to other aluminium alloys. As received aluminium alloy (Al6061) was used for the measurement of the effect of residual stress on microstructure at a surface. It was purchased from Ram Metal Private Limited, New Delhi, India. The deep cold rolled sample is shown in figure 3.1

**Table 3.1:** Chemical composition of Aluminum alloy (Al6061).

Elements	Mg	Si	Fe	Co	Zn	Ti	Mn	Cr	Other	Al
Wt. %	0.8	0.4	0.7	0.15	0.25	0.15	0.15	0.04	0.05	97.31

---



**Figure 3.1:** Deep rolled aluminium (Al 6061) plate.

### 3.3 Methodology

Commercial aluminium alloy (Al6061), with chemical composition listed in Table 3.1, was used. The base material, (300×100mm) with 8 mm thick strip was deep cold rolled at deep rolled depth 0.5 mm, 1 mm, 1.5 mm and 2 mm. The roller with 3-inch diameter and rotating at a uniform rotational speed of 10 rpm was used in the present work. Rolled samples were carefully polished (finishing with sub-micron SiC paper and then electro-polishing) to different deep rolled depth. Controlled electro-polishing was used: an electrolyte of 80:20 methyl alcohol and perchloric acid at 27V, 4.5A current for 10 sec. The residual stresses were measured through grazing incidence X-ray diffraction (GIXRD) technique. The residual stress measurements were made in a Panalytical™ MRD system. In this study, measurements were made for both  $\sigma_{11}$  and  $\tau_{12}$ . A surface microstructure evolution was also characterized through electron backscattered diffraction (EBSD). The EBSD scans were performed in a Quanta 3D FEG (Field emission gun) using a OIM EBSD package software. For each specimen and thickness location, an area of 100 X 100  $\mu\text{m}$  was covered at a step size of 0.1  $\mu\text{m}$ .

### 3.4 Machines and Equipment

#### 3.4.1 Diamond Cutter

Diamond cutter (Make: Struers, Danish) was used for cutting the as-received material of Al 6061 alloy. The size of specimen was so chosen that the length of the sample cut was approximately equal to 4 pieces. Figure 3.2 presents the Diamond cutter setup and Aluminium piece cut by diamond cutter.



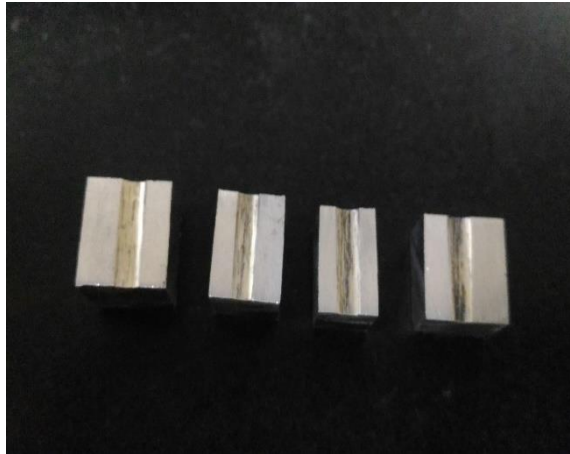


**Figure 3.2:** Diamond cutter (Courtesy: IIT, Bombay) and Cut sample of Al6061.

### 3.4.2 Deep Cold Rolling Setup

Deep rolling set-up was used on horizontal milling machine to deep roll the as-received material aluminium (Al 6061) from 0.5mm, 1mm, 1.5mm and 2mm depth. The rollers of approx. 3" diameter, 5mm width and 2.5mm radius of roller is used were used to deep roll the material. The deep rolling milling machine was carried out at 450 rpm to achieve the desired sample reductions. Figure 3.3 presents the schematic of deep rolling setup.



**Figure 3.3:** Deep rolling setup (Courtesy: Thapar University, Patiala).

### 3.4.3 Tensile Testing Machine

Tensile testing, three samples of Al 6061 at 0°, 45° and 90° (45 mm length) were prepared by Wire EDM according to ASTM standards. The tensile test specimens were subjected to analysis to determine the material property. Figure 3.4 presents the schematic of Tensile testing machine.



**Figure 3.4:** Tensile testing (Courtesy: IIT, Bombay).

### **3.4.4 GIXRD- Grazing Incidence X-Ray diffraction**

The Grazing Incidence X-ray Diffraction (XRD) is a rapid panalytical<sup>TM</sup>, non-destructive system for analyzing a large range of alloys, including metals, polymers and semiconductors. GIXRD method is used for materials investigate the residual stress from a surface at an omega angle (for e.g. 0.1, 0.2, 0.3 etc.). Residual stress measurements for four samples i.e. as received or 0.5mm, 1mm, 1.5mm and 2mm depth at their surfaces at an omega angle 0.1, 0.5 and 0.8 is measured. Figure 3.5 shown a GIXRD panalytical<sup>TM</sup> sample setup.



**Figure 3.5:** GIXRD Panalytical<sup>TM</sup> setup (Courtesy: IIT, Bombay).

### 3.4.5 Polishing

The surface to be examined by EBSD was polished with abrasive papers of successive finer grades such as 400, 800, 1500 and hand polishing at deep rolled groves 2000 mesh abrasive paper and setup of grinding (polishing) is shown in figure 3.6. Each time the sample was rubbed on SiC paper, scratch marks were introduced, therefore polishing was continued till all the scratches were in one direction. Then, the next paper with finer grade was used with direction of rubbing switched perpendicular to previous scratches.



**Figure 3.6:** Abrasive papers and setup of grinding (polishing) (Courtesy: IIT, Bombay).

Similar process was repeated from the coarse grade paper (400 grit size) up to fine grade paper (2000 grit size). Over-heating of sample was avoided so that no modification in the microstructure occurs. Pressure needs to be adjusted, as high pressures can introduce deep scratches whereas low pressures result in long time consumption.

### 3.4.6 Electro-polishing

The electropolishing can be done on prepared samples so as to remove dust and scratches and show a mirror image groove of the samples. Electro-polishing to be done with perchloric acid 20% and methanol 80% at 27V, 4.5A current for 10sec. Figure 3.7 illustrates the precision cutter utilized in the present work.



**Figure 3.7:** Electro-polishing (Courtesy: IIT, Bombay).

### 3.4.7 Wire EDM Set-up

The sample for tensile testing was prepared in wire EDM with 0.5  $\mu\text{m}$  wire diameter for cutting samples Figure 3.8 (Make: Sprintcut734, Navi Mumbai).



**Figure 3.8:** Wire EDM (Courtesy: IIT, Bombay).

### 3.4.8 Electron Back Scatter Diffraction (EBSD)

Electron back scatter diffraction was performed to measure orientation, texture measurement, grain size and boundary types of Al6061 to find the effect residual stress on microstructure. Figure 3.9 presents the schematic for EBSD.

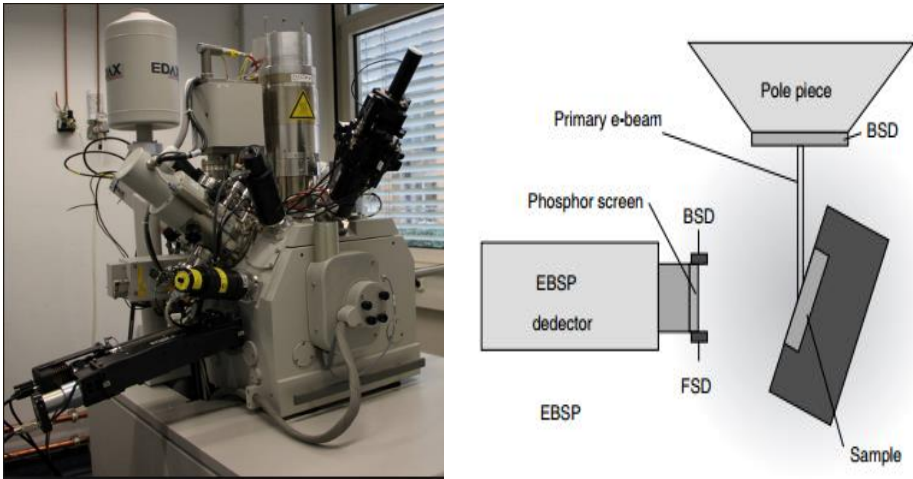


**Figure 3.9:** EBSD setup (Courtesy: IIT, Bombay).

### 3.4.9 Surface Roughness Testing:

To determine the surface roughness of specimens, surface roughness tester was used. The surface roughness test was done at Thapar University, Patiala. The surface roughness tester machine was made by Mitutoyo (Japan). And  $0.01\mu\text{m}$  is the least count of the surface roughness. It is calibrated by the vertical deviation of a real surface from its ideal form. If these deviations are broad, then the surface is rough; if these deviations are less the surface is smooth. Roughness is typically considered to be the, short wavelength, high frequency component of a measured surface. Surface roughness is generally a good predictor of the performance of a mechanical component. And surface roughness testing machine was used to measure average surface finishing or roughness ( $R_a$ ) of a sample Al 6061 As received, 0.5mm, 1mm, 1.5mm and 2mm. Stylus is scanning a sample and measure surface roughness ( $R_a$ ) value. And these value show in digital meter whose connected with stylus. a setup of surface roughness testing machine is shown in figure 3.10.

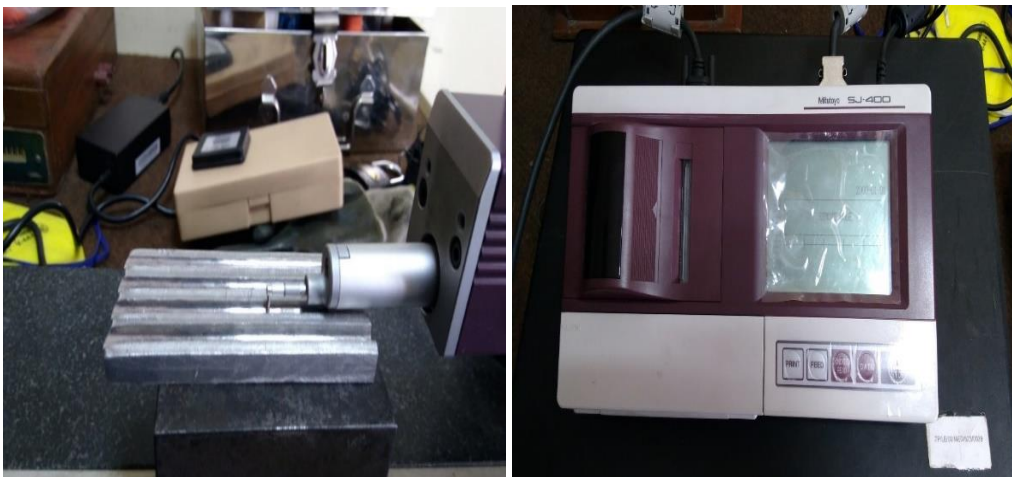




**Figure 3.10:** Surface Roughness Testing Machine (Courtesy: Thapar University, Patiala).

### **3.5 Summary of this chapter**

This chapter describes the objective, methodology, and equipment used for the experimental work. In the last section, details of different instruments and facilities that played a major role in the characterisation of as received material.

# Chapter 4

## Finite Element Modelling

---

### 4.1 Physical Description of the FE Model

A three dimensional, Elasto-plastic finite element model was developed for deep cold rolling. The simulations were conducted in Abaqus™, a commercial simulation package. Abaqus™ gives an easy, interface for creating and verifying results with simulations. Abaqus™ is subdivided into units, each unit defines phase of the modeling; for example, geometry definition, defining properties of material, and generate meshing. As the move from unit to unit, you make the model and generates files that will submit to the Abaqus™ for analysis. This analysis, moves information to Abaqus™ to check the progress of jobs submitted, and creates an output file. Finally, the visualization unit of Abaqus™ to read the completed job and view the results of the analysis. In this experiment, an elastic plastic deformable rectangular titanium sheet 150 mm in length, 100 mm in width and 8mm thickness is deep rolled by deep rolling roller. A deep rolling roller were 3-inch in diameter, 5 mm in thickness, 2.5 mm round at upper and having a uniform rotational speed of 10 RPM. A roller was modelled as discrete rigid and the sheet was taken as an elastic-plastic body. The experiment as well as simulations were conducted for 0.5 mm, 1 mm, 1.5 mm and 2 mm depth from top surface deformation is shown in figure 4.1. An Elasto-plastic model was used in the present study to calculate the residual stress distribution on the upper deep rolled surface during deep cold rolling. In Abaqus™ we have implicit and explicit techniques for simulation. The implicit method requires more time than explicit. Also, the implicit method is competent in determining static problems, but it is not appropriate for large deformation problems such as deep cold rolled. Hence the explicit method was used for the simulation as it takes less time to calculate the results. Simulations were performed one for 0.5 mm and then 1 mm, 1.5 mm, 2 mm deep rolled from the top surface. Frictional contact between the roller and the sheet is maintained. Coulomb friction was given to the contact surfaces and it is important to note that adequate friction is required to contact between the sheet and deep roller. Frictional forces at the interface of the roller and the sheet is responsible for pulling the sheet through the roller. In the entry zone, a roller moves faster than the sheet whereas in the exit zone, the roller rotational velocity is same as the sheet traverse velocity. A residual stress gradient has been observed at the surface of the deep rolled sheet.

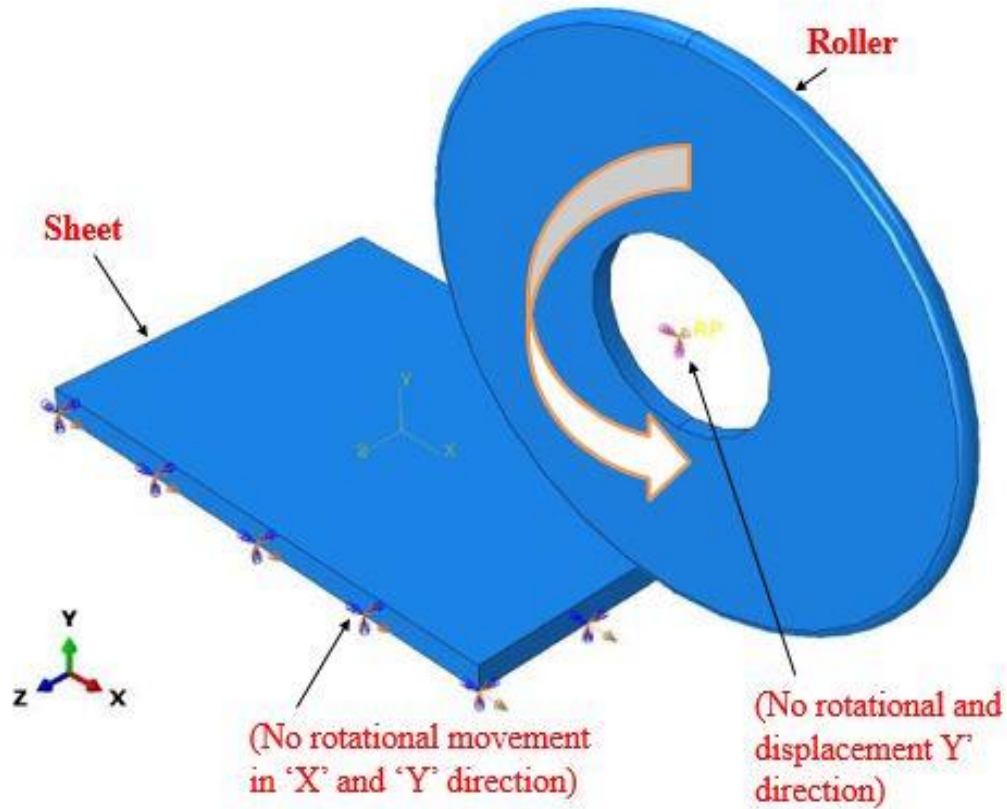


**Figure 4.1:** A three dimensional, Elasto-plastic finite element model for 0.5 mm, 1 mm, 1.5 mm and 2 mm deep rolled.

## 4.2 Numerical Formulation

The geometric model was using continuum stress/displacement, 8-nodded linear brick, and (C3D8R elements). A structured mesh was used in this model. Abaqus/Explicit has three different options for C3D8R elements i.e average strain kinematic, orthogonal and centroid formulations. The average strain kinematic formulation has been used in this study. Though, average strain kinematic formulation required more computational time compared to other two formulation technique. It was preferred due to more accuracy of the results. An optimum meshing (sweep quad-dominated) is required for proper computational time. The solid model used in this study had 56250 elements and 58420 nodes with 15 elements in thickness and 250 elements in the width direction. For reduction of time, a non-uniform meshing was generated in the thickness direction using double biasing with a bias ratio of 3 as shown in Figure 4.2.

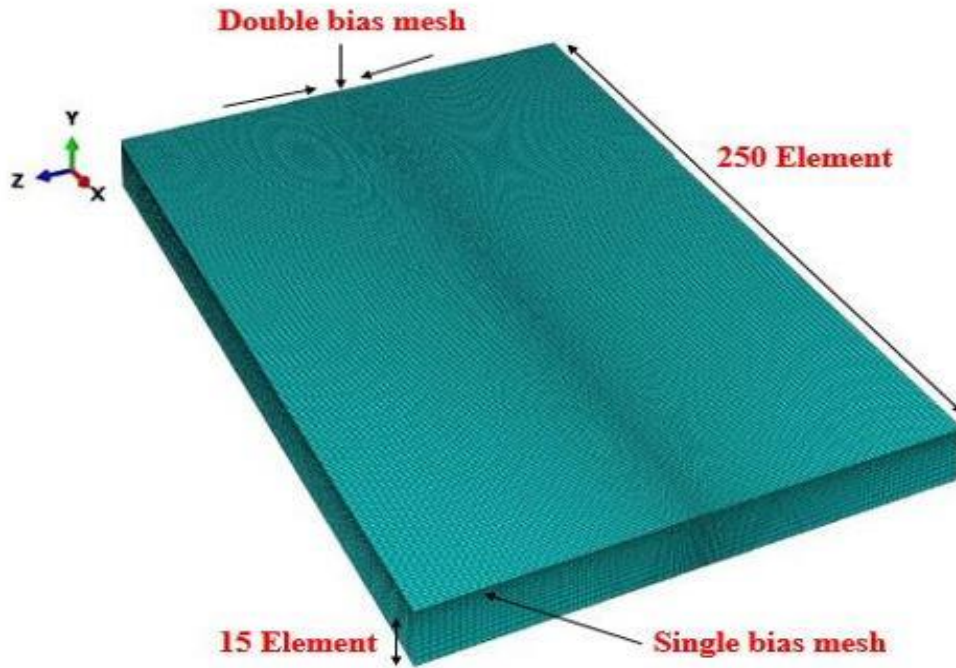


**Figure 4.2:** Meshing of sheet.

### 4.3 Material model

For the isotropic model, Young's modulus of elasticity ( $E$ ) and Poisson's ratio ( $\nu$ ) were taken to be 68.9 GPA and 0.33, respectively. The plastic data were used in a tabular form as seen in Table 4.3 to define the flow stress model, which follows the stress-strain curve behaviour as shown in Figure 4.4.

**Table 4.1:** Plastic flow stress.

Yield Stress	Plastic Strain
75	0
78	0.05
87.5	0.20
82.7	0.35
68	0.47

### 4.4 Boundary and contact conditions

Boundary conditions were divided into two steps; an initial step and the analysis step. In the initial step, the sheet was given an initial velocity of 10 mm/s in 'x' direction. The interaction between the roller and the upper surface of the sheet was defined in this step. A

displacement/rotation boundary condition was defined to constrain the motion of the sheet. The side faces of the sheet are made zero in 'y' and 'z' direction. Similarly, the boundary condition of the roller was made such that the roller could rotate only about their respective axis of rotation. All other translational and rotational degrees of freedom were constrained in 'x' and 'z' directions as shown in Figure 4.1. In the analysis step, the rollers were given with an equal and opposite angular velocity. The friction model used in this study, allows the relative motion between the two contact surfaces. The frictional coefficient values used in the simulations is 0.2.

## 4.5 Mesh Sensitivity

Element size plays an important role in attaining accurate results. The large number of elements can increase the computational time and a very small number of elements can lead to the inaccurate results. Therefore, determining the optimal element size is must for carrying out the simulation effectively. Simulations were done using different mesh sizes and the number of elements in the model ranged between 50000 and 60000. It can be seen in Figure 4.3 that the maximum stress values saturate at 56250 elements.

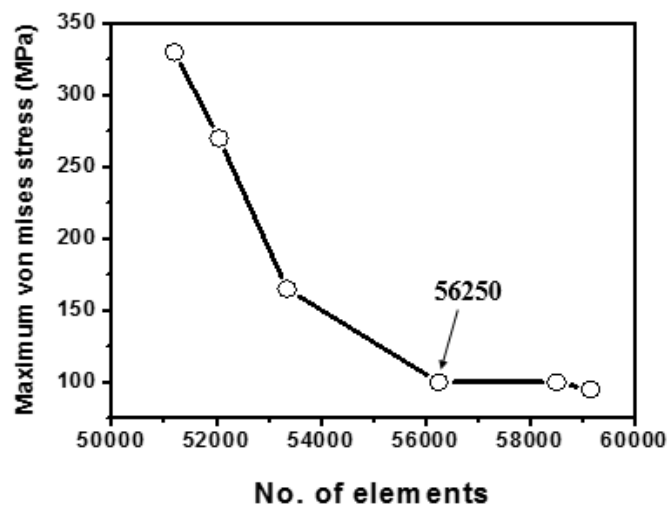


Figure 4.3: Mesh sensitivity analysis.

# Chapter 5

## Results and Discussion

---

### 5.1 Introduction

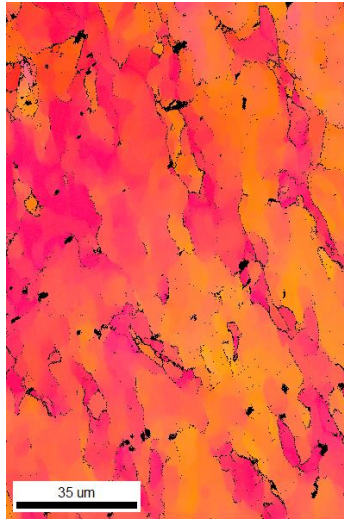
This chapter is divided in two parts. In first part define the experimental results and second part illustrate FEM simulations and their comparison with experimental results. This chapter presents the characterization and testing results obtained for Aluminium alloy (Al6061). And describe the various EBSD, residual stress and surface roughness analysis obtained for as received Al6061 and different deep rolled depth 0.5mm, 1mm, 1.5mm and 2mm material at a different penetration depth of 0, 0.15, 0.3, 0.45 and 0.6 mm from top surface of the deep rolled specimen.

### 5.2 Surface Microstructural Development

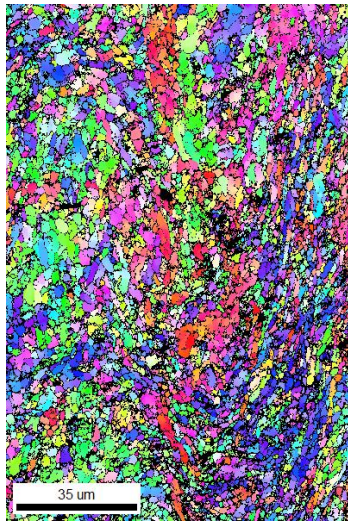
At a surface, microstructural developments are described in terms of gradients in grain structure and residual stress. These are shown one by one in below.

#### 5.2.1 Gradients in Grain Structure:

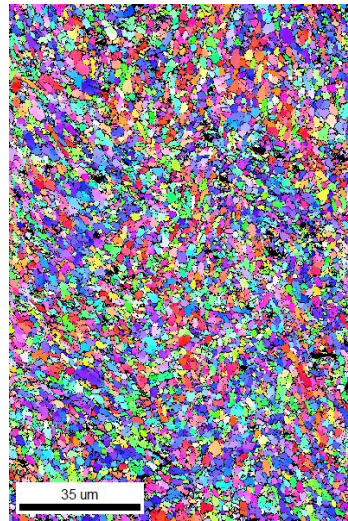
From the figure (5.1) it can be clearly observed finest grain size was produced when deep rolled depth at a 2mm. And the grain size started increasing when the deep rolled depth was reduce. As Larger grain size was observed when deep rolled at 0.5mm as compare to other deep rolled depth. Also, the material plastic flow increase as a deep cold rolled depth increases from 0.5 to 2mm.



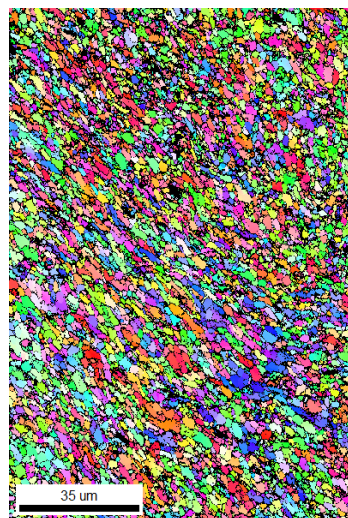
(AR)



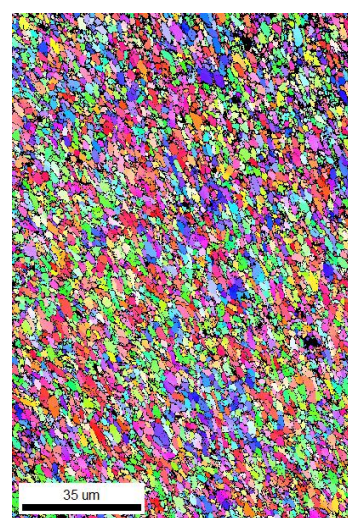
(0.5mm)



(1mm)



(1.5mm)



(2mm)

**Figure 5.1:** EBSD results.

The EBSD data were analysed to get indication of the deep rolling induced deformation gradients in grain size (Fig. 5.2a). Grain size reduced with increasing deep rolling depth from 0.5 to 2 mm. When increased rolling depth up to 2mm is lead to elongation of grains and increased the fraction of the non-indexed points. After EBSD it clearly depicts that the grain size as received material (135.89  $\mu\text{m}$ ) were large but when the specimen was deep cold rolled the grain size drastically decreased (from 135.89  $\mu\text{m}$  to 3.11  $\mu\text{m}$ ) becomes finer and afterwards it changes to 1.95  $\mu\text{m}$  as shown in figure 5.2a. Finer the grain size better the fatigue strength of a material. The indication of the surface deformation gradients were also observed on the local misorientation developments (see Fig. 5.2b) for the kernel average misorientation (KAM).

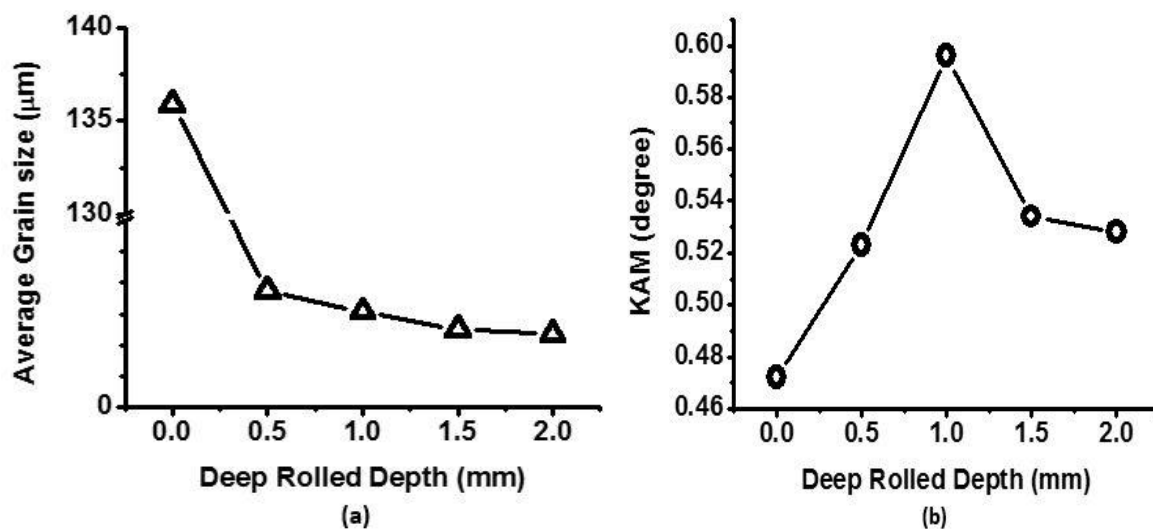


**Figure 5.2:** EBSD data for different deep rolled depth 0, 0.5, 1, 1.5, 2 mm (a) Grain size and (b) kernel average misorientation (KAM).

### 5.2.2 Gradients in residual stress:

The multiple GIXRD method was used to determine the experimentally residual stress development at a surface and sub surface of the deep cold rolled specimen. As mentioned in 3<sup>rd</sup> chapter, this method considered all the available  $\{hkl\}$  poles for determining the both normal ( $\sigma_{11}$ ) and shear ( $\tau_{12}$ ) components of the stress matrix. The stress distribution across the sheet thickness for different deformation percentage is plotted in Fig. 5.2.

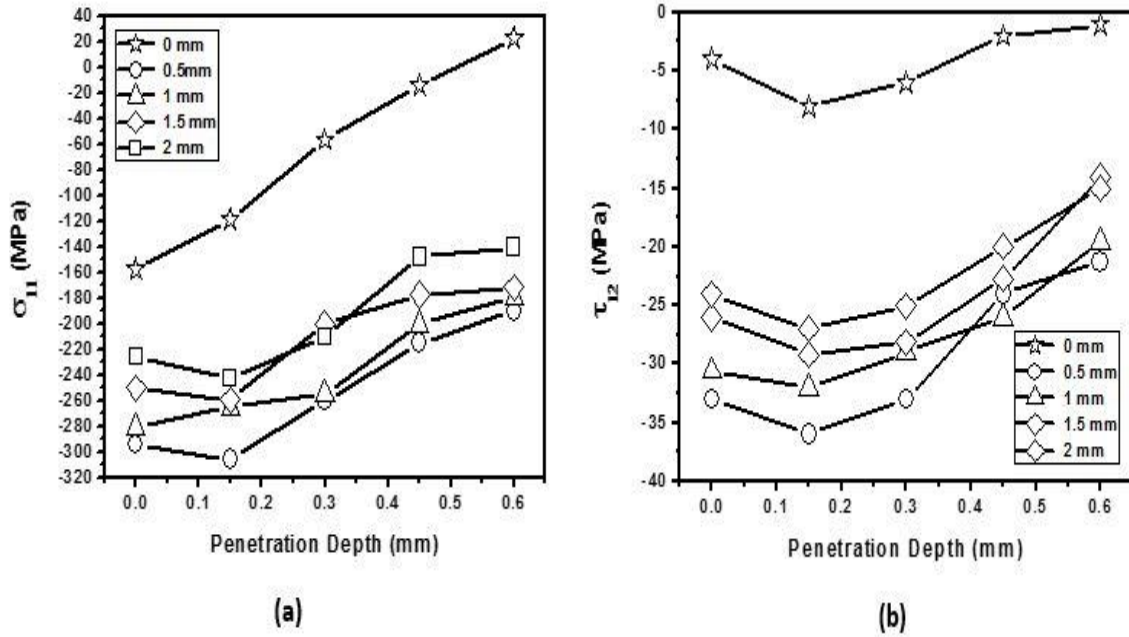


**Figure 5.3:** Residual stress signatures as a function of thickness: (a)  $\sigma_{11}$  and (b)  $\tau_{12}$ .

From the figure 5.3a it can be clearly seen that a particular deep rolled state in a longitudinal direction, residual stress on the surface of the material is less as compare to residual stress generated over the sub-surface. Moreover, as we move beyond sub surface the compressive residual stress starts decreasing. Same trend was reported by Beghini et al.[18]. However, if we change the deep rolled state to 2 mm it can be observed that at any particular penetration depth in the graph the values of compressive residual stress is less as compare to residual stress developed at deep rolled state of 0.5 mm. Due to such difference in values of residual stresses a gradient generates from -305 MPa to -180.3 MPa. A highly compressive residual stress (-305MPa) has been observed on the surface (on top surface) of the specimen which changes to (-180MPa) and further a reduction in stress was observed afterwards (see Fig. 5.3a). From the figure 5.3b it can be clearly understood that a particular deep rolled state, shear stress on the surface of the material is less as compare to residual stress generated over the sub-surface. Furthermore, if we change the deep rolled state to 2mm it can be observed that at any particular penetration depth in the graph the values of shear stresses are slightly less as compared to shear stresses developed at deep rolled state of 0.5mm. Therefore, the value of deformation gradient could be considered as negligible. A highly compressive residual stress (-33.78MPa) has been observed on the surface (0.0mm penetration depth) of the specimen which changes to (-18.59MPa) and further a reduction in stress was observed afterwards (see Fig. 5.3b).

## 5.3 Process Characterization via Finite Element Simulations

### 5.3.1 Evolution surface residual stresses

From the figure 5.4 it can be clearly seen that a particular deep rolled state in a longitudinal direction (LD), residual stress on the surface of the material is less as compare to residual stress generated over the sub-surface. Moreover, as we move beyond sub surface the compressive residual stress starts decreasing. However, if we change the deep rolled state to 2mm it can be observed that at any particular penetration depth in the graph the values of compressive residual stress are less as compare to residual stress developed at deep rolled state of 0.5mm. Due to such difference in values of residual stresses a deformation gradient generates from -305MPa to -180.3MPa. A highly compressive residual stress (-350MPa) has been observed on the surface (0 mm penetration depth) of the specimen which changes to (-180MPa) and further a reduction in stress was observed afterwards (see Fig. 5.4).

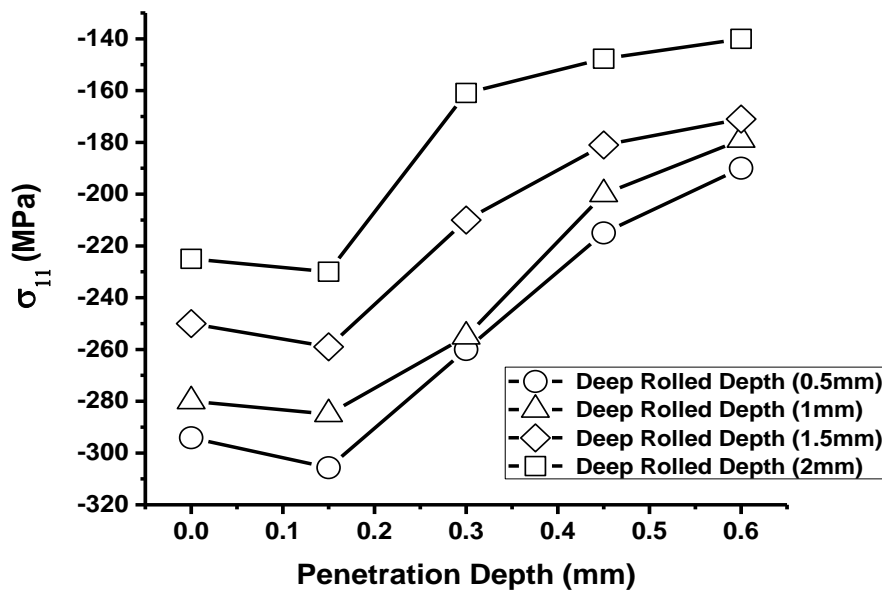


Figure 5.4: Residual stress gradient in longitudinal direction (LD).

From the figure (5.5) it can be clearly seen that a particular deep rolled state in a transverse direction (TD), compressive residual stress on the surface of the material is maximum and its values start decreasing as the penetration depth increases. Moreover after 0.4mm penetration depth, the nature of residual stress changes form compressive to tensile. A highly compressive residual stress (-184.32MPa) has been observed on the surface (0 mm

penetration depth) of the specimen which changes to (12.2MPa) and further a reduction in stress was observed afterwards (see Fig. 5.5).

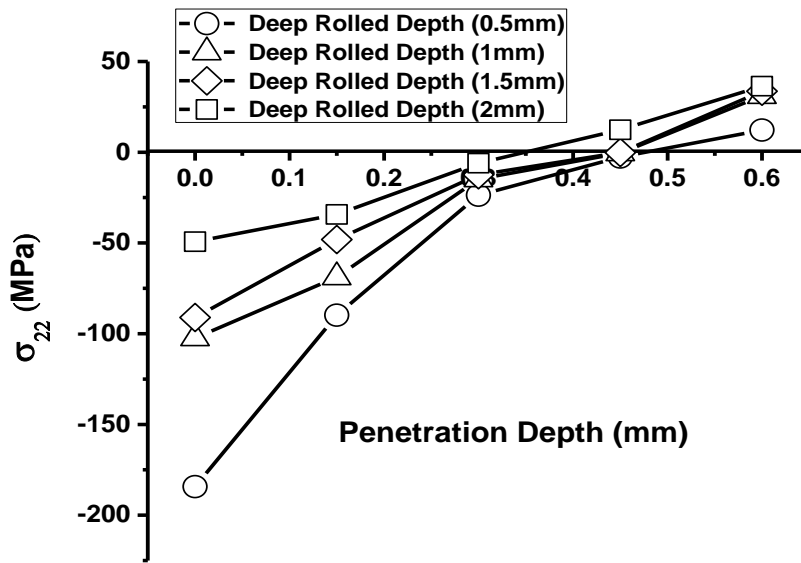


Figure 5.5: Residual stress gradient in transverse direction (TD).

From the figure (5.6) it can be clearly understood that a particular deep rolled state, shear stress on the surface of the material is less as compare to residual stress generated over the sub-surface. Furthermore, if we change the deep rolled state to 2mm it can be observed that at any particular penetration depth in the graph the values of shear stresses are slightly less as compared to shear stresses developed at deep rolled state of 0.5mm. Therefore, the value of deformation gradient could be considered as negligible. A highly compressive residual stress (-35.32MPa) has been observed on the surface (0.0mm penetration depth) of the specimen which changes to (-21.29MPa) and further a reduction in stress was observed afterwards (see Fig. 5.6).

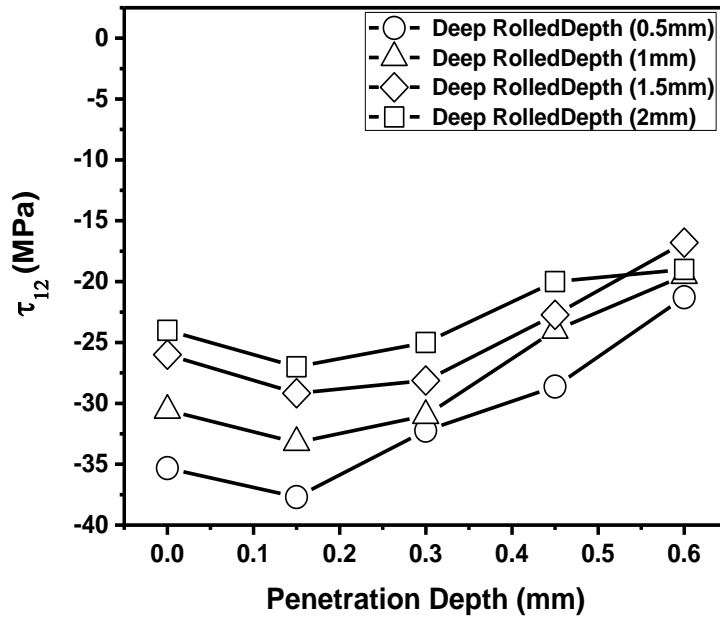


Figure 5.6: Shear stress gradient.

From figure (5.7) it can be observed that at the beginning of deep cold rolling the reaction force was least and it started to increase with increase in time. As the roller is about to cross the sheet there is a slight decrease in reaction force and further as it passes completely the sheet the reaction force becomes constant. At a particular time the reaction force increases as the deep rolled depth increases from 0.5 to 2mm.

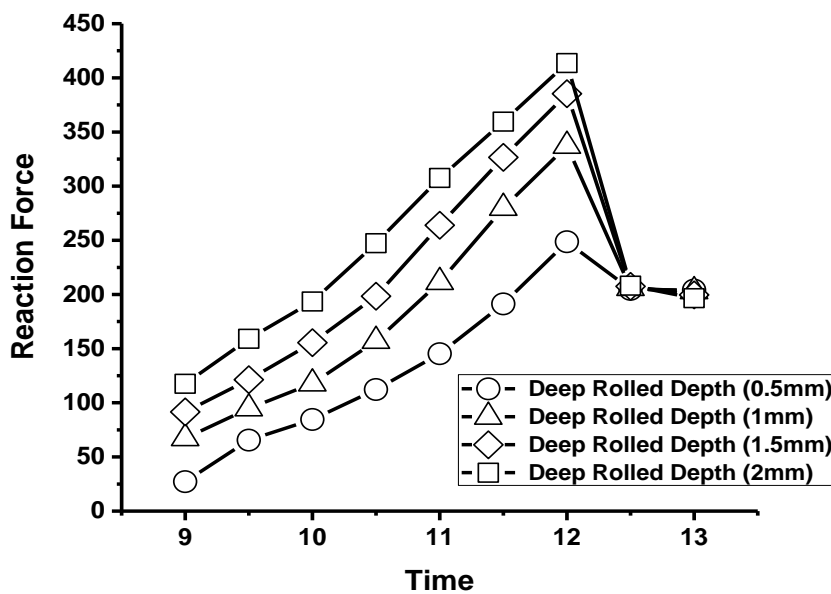


Figure 5.7: Relationship of reaction force with time.

### 5.3 Surface roughness

In deep rolling process, the average surface roughness value decreases drastically from 0mm to 0.5mm deep rolled depth and it goes further surface roughness value become constant from 0.5mm to 1.5mm as shown in figure 5.8. And as again depth rolled depth increases, there is slight increase in the average surface roughness value because with the increase of depth thickness deep rolled force increase. Which causes crack propagation over the surface and its effect the surface finish of the specimen. Thus, from the graph we can conclude that deep rolling process gives better surface finish in range of 0.5 to 1.5mm deep rolled depth.

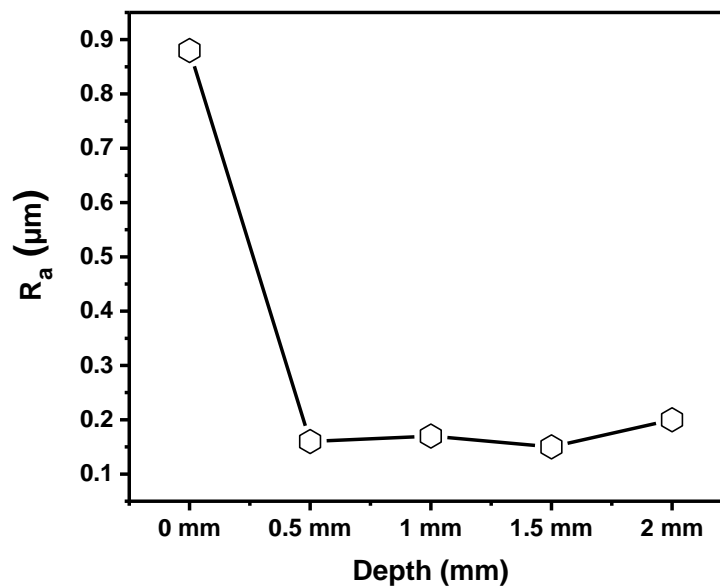


Figure 5.8: Average surface roughness.

# Chapter 6

## Conclusion and Scope of Future Work

---

### 6.1 Conclusions

This chapter concludes the results obtained from experiments performed during the present research. Initially, the results obtained from microstructure and residual stress analysis was discussed. Aluminium sheet (of 8 mm thickness) was deep rolled at a depth 0.5 mm, 1 mm, 1.5 mm and 2 mm. Experimental measurements were made at a surface evolution in microstructure and residual stress. Numerical simulations were made at surface gradients in residual stresses. Following are the main observations:

1. Comparison between the simulated and experimental measurements was possible for the residual stress. Both experiments and simulations showed similar trends near surface compressive residual stresses.
2. Grain structure (grain size, grain misorientation) showed a clear gradient at the surface.

### 6.2 Scope of future work

1. Correlation between texture development and residual stress distribution.
2. Effect of tool geometry on the surface of residual stress gradient.
3. Effect of compressive residual stress, surface roughness and surface hardness on corrosion rate during deep rolling can be studied in near future.

# References

---

1. Majzoobi, G.H.; Azadikhah, K.; Nemati, J. (2009) The effects of deep rolling and shot peening on fretting fatigue resistance of Aluminum-7075-T6. *Materials Science and Engineering: A*, 516(1): 235-247.
2. Residual stress info. *Proto manufacturing*, <http://www.protoxrd.com/residual-stress-info.html> (accessed on – 23/11/2016).
3. Manouchehrifar, A.; Alasvand, K. (2009) Finite element simulation of deep rolling and evaluate the influence of parameters on residual stress. *Recent Researches in Engineering Mechanics, Urban & Naval Transportation and Tourism*, ISBN: 978-1-61804-078-7
4. Automated XRD system and services. *proto manufacturing* [www.protoxrd.com](http://www.protoxrd.com) (accessed on – 23/05/2017).
5. Verlinden, B.; Driver, J.; Samajdar, I.; Doherty, R.D. (2007) Thermo-mechanical processing of metallic materials. *Pergamon Materials Series* (Vol. 11). ISBN: 978-0-08-044497-0
6. Understanding stress and strain. *Material science and Engineering* <http://home.iitk.ac.in/~anandh/E-book.htm>, (accessed on – 23/05/2017).
7. Chatterjee, K.; Venkataraman, A.; Garbaciak, T.; Rotella, J.; Sangid, M. D.; Beaudoin, A. J.; Pilchak, A. L. (2016). Study of grain-level deformation and residual stresses in Ti-7Al under combined bending and tension using high energy diffraction microscopy (HEDM). *International Journal of Solids and Structures*, 94: 35-49.
8. Yentzer, T.; Stillman, B. Stillman (1999) Fatigue Life and Residual Stresses in Cold Rolled Propeller Blades. *Conference on Aging Aircraft, Albuquerque, NM*
9. Liouand, T.I.; Wardany, E.I.; Finite Element Analysis of Residual Stress in Ti-6Al-4V Alloy Plate Induced by Deep Rolling Process under Complex Roller Path. *International Journal of Manufacturing Engineering*. <http://dx.doi.org/10.1155/2014/786354>.
10. Wong, C. C.; Hartawan, A.; Teo, W. K. (2014). Deep cold rolling of features on aero-engine components. *Procedia CIRP*, 13: 350-354.
11. [http://www.aluminiumleader.com/history/industry\\_history/](http://www.aluminiumleader.com/history/industry_history/) (accessed on - 17/07/2017)
12. <https://en.wikipedia.org/wiki/Aluminium> (accessed on - 17/07/2017)

13. Schuren J. (2006) Al 7075 T6: Mechanical Properties, Microstructure Evolution and Residual Stresses, MSE 610
14. <https://www.metalsupermarkets.com/metals/aluminum/alloys/> (accessed on 17/07/2016)
15. <http://www.constellium.com/technology-center/aluminium-alloy-properties> (accessed on - 13/07/2017)
16. Altenberger I. (2005) deep rolling - the past, the present and the future
17. Beghini, M.; Bertini, L.; Monelli, B. D.; Santus, C.; Bandini, M. (2014) Experimental parameter sensitivity analysis of residual stresses induced by deep rolling on 7075-T6 aluminium alloy. *Surface and Coatings Technology*, 254: 175-186.
18. Zhuang, W.; Liu, Q.; Djugum, R.; Sharp, P. K.; Paradowska, A. (2014) Deep surface rolling for fatigue life enhancement of laser clad aircraft aluminium alloy. *Applied Surface Science*, 320: 558-562.
19. Altenberger, I.; Wagner, L.; Mhaede, M.; Juijerm, P.; Noster, U. (2008) Effect of deep rolling on the cyclic performance of magnesium and aluminum alloys in the temperature range 20–250 C. *Proceedings of the 10th International Conference on Shot Peening (ICSP), ACMU, Tokyo, Japan.*
20. Kloos, K. H.; Fuchsbauer, B.; Adelman, J. (1987) Fatigue properties of specimens similar to components deep rolled under optimized conditions. *International journal of fatigue*, 9(1): 35-42.
21. Eigenmann, B., Holzwarth, U., Kachler, W., & Goske, J. (2005). Deep Rolling of Titanium Rods for Application in total Hip Arthroplasty. *9th International Conference on Shot Peening in Paris.*
22. Juijerm, P., & Altenberger, I. (2012). Effects of Deep Rolling and Its Modification on Fatigue Performance of Aluminium Alloy AA6110. In *Aluminium Alloys-New Trends in Fabrication and Applications.*
23. Rossini, N. S., Dassisti, M., Benyounis, K. Y., & Olabi, A. G. (2012). Methods of measuring residual stresses in components. *Materials & Design*, 35: 572-588.
24. Ye, N. Y., Cheng, M., & Zhang, S. H. (2015). Effect of Cold Rolling Parameters on the Longitudinal Residual Stress Distribution of GH4169 Alloy Sheet. *Acta Metallurgica Sinica (English Letters)*, 28(12): 1510-1517.
25. <http://.residualstress.org> (25/11/2016)